

# EANM/ESC procedural guidelines for myocardial perfusion imaging in nuclear cardiology

B. Hesse<sup>1</sup>, K. Tägil<sup>2</sup>, A. Cuocolo<sup>3</sup>, C. Anagnostopoulos<sup>4</sup>, M. Bardiés<sup>5</sup>, J. Bax<sup>6</sup>, F. Bengel<sup>7</sup>, E. Busemann Sokole<sup>8</sup>, G. Davies<sup>9</sup>, M. Dondi<sup>10</sup>, L. Edenbrandt<sup>2</sup>, P. Franken<sup>11</sup>, A. Kjaer<sup>1</sup>, J. Knuuti<sup>12</sup>, M. Lassmann<sup>13</sup>, M. Ljungberg<sup>14</sup>, C. Marcassa<sup>15</sup>, P. Y. Marie<sup>16</sup>, F. McKiddie<sup>17</sup>, M. O'Connor<sup>18</sup>, E. Prvulovich<sup>19</sup>, R. Underwood<sup>20</sup>, B. van Eck-Smit<sup>8</sup>

<sup>1</sup> Department of Clinical Physiology and Nuclear Medicine, Rigshospitalet, University Hospital of Copenhagen, Copenhagen, Denmark

<sup>2</sup> Department of Clinical Physiology, Malmö University Hospital, Malmö, Sweden

<sup>3</sup> Department of Biomorphological and Functional Sciences, University Federico II, Naples, Italy

<sup>4</sup> Imperial College School of Medicine (NHLI), London, UK

<sup>5</sup> INSERM U601, Nantes, France

<sup>6</sup> Department of Cardiology, Leiden University Medical Center, Leiden, The Netherlands

<sup>7</sup> Nuklearmedizinische Klinik der TU, Munich, Germany

<sup>8</sup> Department of Nuclear Medicine, Academic Medical Center, Amsterdam, The Netherlands

<sup>9</sup> Department of Medical Physics, Hull and East Yorkshire Hospitals NHS Trust, Hull, UK

<sup>10</sup> Nuclear Medicine Section, Division of Human Health, International Atomic Energy Agency, Vienna, Austria

<sup>11</sup> Nuclear Medicine, AZ VUB, Brussels, Belgium

<sup>12</sup> Turku PET Centre, Turku University Central Hospital, Turku, Finland

<sup>13</sup> Klinik für Nuklearmedizin, Universität Würzburg, Würzburg, Germany

<sup>14</sup> Department of Medical Radiation Physics, The Jubileum Institute, Lund, Sweden

<sup>15</sup> Fondazione Maugeri, IRCCS, Verona, Italy

<sup>16</sup> Service de Médecine Nucléaire, Hôpital de Brabois, Vandoeuvre, France

<sup>17</sup> Nuclear Medicine Department, Aberdeen Royal Infirmary, Foresterhill Scotland, UK

<sup>18</sup> Section of Nuclear Medicine, Mayo Clinic, Rochester MN, US

<sup>19</sup> Institute of Nuclear Medicine, Middlesex Hospital, London, UK

<sup>20</sup> Department of Nuclear Medicine, Royal Brompton Hospital, London, UK

Published online: 21 May 2005

© Springer-Verlag 2005

**Abstract.** The European procedural guidelines for radionuclide imaging of myocardial perfusion and viability are presented in 13 sections covering patient information, radiopharmaceuticals, injected activities and dosimetry, stress tests, imaging protocols and acquisition, quality control and reconstruction methods, gated studies and attenuation-scatter compensation, data analysis, reports and image display, and positron emission tomography. If the specific recommendations given could not be based on evidence from original, scientific studies, we tried to express this state-of-art. The guidelines are designed to assist in the practice of performing, interpreting and reporting myocardial perfusion SPET. The guidelines do not discuss clinical indications, benefits or drawbacks of radionuclide myocardial imaging compared to non-nuclear techniques, nor do they cover cost benefit or cost effectiveness.

**Abbreviations** AC: Attenuation compensation (attenuation correction) · ALS: Advanced life support · COR: Centre of rotation · DRL: Diagnostic reference levels · EF: Ejection fraction · FBP: Filtered back-projection · FDG: Fluorodeoxyglucose · FWHM: Full-width at half-maximum · LEAP: Low-energy, all-purpose (collimator) · LEGP: Low-energy general-purpose (collimator) · LEHR: Low-energy high-resolution (collimator) · LV: Left ventricular · LVEF: Left ventricular ejection fraction · MLEM: Maximum likelihood expectation maximisation · NEMA: National Electrical Manufacturers Association · OSEM: Ordered subsets expectation maximisation · PVC: Premature ventricular contractions · QC: Quality control · SA block: Sinoatrial block · SDS: Summed difference score · SRS: Summed rest score · SSS: Summed stress score ·

B. Hesse (✉)

Department of Clinical Physiology and Nuclear Medicine, Rigshospitalet, University Hospital of Copenhagen, Copenhagen, Denmark  
e-mail: bhesse@rh.hosp.dk

**Eur J Nucl Med Mol Imaging (2005) 32:855–897**  
DOI 10.1007/s00259-005-1779-y

## Preamble

The European procedural guidelines for radionuclide myocardial perfusion imaging (MPI) have been developed by the “Guidelines Group” of the European Council on Nuclear Cardiology (joint group of the European Association of Nuclear Medicine and of the European Society of Cardiology). The guidelines are intended to present information specifically adapted to European practice, based on evidence from original scientific studies or on previously published guidelines (European national guidelines for MPI and the European Society of Cardiology and ACC/AHA guidelines, as well as U.S. guidelines for MPI and nuclear cardiology procedures [see references 1–5 in reference list in Guidelines: Anagnostopoulos et al. in *Heart* 2004;90:i1–10; ESC Guidelines for Exercise Testing; The ACC/AHA Exercise Testing Guidelines; Society of Nuclear Medicine; American Society of Nuclear Cardiology] or on expert consensus. Where more than one solution seems to be practised, and none has been shown to be superior to the others, we hope that we have succeeded in specifically expressing this state of knowledge.

In recent years, radionuclide imaging technologies have evolved rapidly (with the development of new instrumentation and new agents), and both the number and the complexity of choices for the clinician have increased. The aim of the authors has been to document the state-of-the-art applications and protocols approved by experts in the field and to disseminate this information to the European nuclear cardiology community. The guidelines are designed to assist physicians and other healthcare professionals in performing, interpreting and reporting radionuclide tomographic imaging examinations of myocardial perfusion. The guidelines do not discuss overall clinical indications for myocardial SPECT or PET or the benefits and drawbacks of radionuclide myocardial perfusion imaging compared with non-nuclear techniques, nor do they cover cost-benefit or cost-effectiveness aspects in diagnosis or prognosis.

The authors comprise scientists from many different countries, all with sub-speciality expertise in nuclear cardiology. Every effort has been made to avoid conflicts of interest arising from non-academic and non-clinical relationships.

## List of contents

1. Patient information
2. Radiopharmaceuticals
3. Injected activities, dosimetry and radiation exposure
4. Stress tests
5. Imaging protocols
6. Image acquisition
7. Quality control
8. Reconstruction methods
9. Gated myocardial perfusion imaging
10. Attenuation and scatter compensation
11. Data analysis

12. Reports, image display
13. Positron emission tomography

## 1. Patient information

Written information should be provided to patients (or their relatives) in relation to scheduling, and in addition, oral information should be provided on the day of the procedure. Variations will depend on local traditions and regulations. General information to be conveyed to (or obtained from) the patient may include:

- The purpose of the test and a brief description of the procedure (e.g. type of stress test, duration of imaging and the need for the patient to remain in one position under a rotating camera).
- Information about the time(s) and date(s) and the duration of the examination. Advice on giving notice in advance if the patient is unable to attend.
- An informed consent form, to be signed and collected according to local regulations.
- Previous examinations: clinical data and previous relevant cardiovascular examinations must be available before the study. In some countries, it may be relevant to ask patients to bring previous medical records and previous test results.
- Insurance: patients with private insurance should bring all insurance details. Contact with the insurance company should be made beforehand to confirm that they will meet the full cost of the scan.
- Side-effects: some centres prefer to describe side-effects in detail, in particular possible side-effects of stress test(s); other centres do not.
- The report describing the results of the test: this will be sent to the referring physician (and in some countries also to the patient); if possible the time required for delivery of the report should be estimated.

### *Patient preparation*

Heavy meals should be avoided before a stress test. Medications that may interfere with responses to a stress test (anti-anginal drugs, persantine) should be withdrawn, and the patient should abstain from caffeine-containing drugs and beverages (cf. Sect. “[Stress tests](#)”).

### *Radiation exposure*

Risks for the patient and accompanying persons may be described in more or less detail according to rules and traditions. Examples of such information are: The radioactive isotope injected for the study produces less radiation than x-ray procedures such as a CT scan or a kidney study. The isotope given is non-allergenic. The isotope is eliminated from the body quickly through natural decay and waste removal.

*Pregnancy, lactation.* Before radioactivity is injected, specific information must be obtained in pregnant and lactating women and in women of child-bearing age who may be pregnant. Cf. Sect. “[Injected activities, dosimetry and radiation exposure](#)”.

Information is also available at:

- <http://www.quantum-imaging.co.uk>
- <http://www.eanm.org>.

## 2. Radiopharmaceuticals

For perfusion imaging with SPECT, thallium-201 ( $^{201}\text{Tl}$ ) and two technetium-99m ( $^{99\text{m}}\text{Tc}$ ) labelled radiopharmaceuticals (sestamibi and tetrofosmin) are available commercially. Regarding perfusion tracers for positron emission tomography, see Sect. “[Positron emission tomography](#)”

### *Thallium-201*

$^{201}\text{Tl}$  is a commonly used radionuclide for myocardial perfusion studies. It decays by electron capture to mercury-201, emitting mainly X-rays of energy 67–82 keV (88% abundance) and gamma photons of 135 and 167 keV (12% abundance) [6]. It is administered intravenously as thallos chloride and the usual activity is 80 MBq. Following intravenous injection, approximately 88% is cleared from the blood after the first circulation [6], with almost 4% of the injected activity localising in the myocardium. Approximately 60% enters the cardiac myocytes using the sodium–potassium ATPase-dependent exchange mechanism, and the remainder enters passively along an electro-potential gradient. The extraction efficiency is maintained under conditions of acidosis and hypoxia and only when myocytes are irreversibly damaged is extraction reduced [7]. Myocardial uptake of  $^{201}\text{Tl}$  increases proportionately with perfusion when perfusion increases up to 2–2.5 times above the baseline levels and then there is a plateau in myocardial uptake.  $^{201}\text{Tl}$  is initially distributed after intravenous injection to the myocardium according to myocardial perfusion and viability. After initial uptake, prolonged retention depends on the intactness of cell membrane and hence on viability. It redistributes from this distribution over several hours, thus allowing redistribution images to be acquired that are independent of perfusion and reflect viability alone.

$^{201}\text{Tl}$  is a good tracer of myocardial perfusion and it has been used clinically for more than two decades. It does, however, have limitations:

- Relatively long physical half-life: high radiation burden for the patient (80 MBq delivers an effective dose of 18 mSv, somewhat higher than that during coronary angiography).
- Relatively low injected activity: low signal-to-noise ratio; images can be suboptimal (obese patients) and low

count levels impair high-quality ECG-gated SPECT studies.

- Relatively low energy emission: low-resolution images and significant attenuation by soft tissue.

$^{99\text{m}}\text{Tc}$  compounds do not have these limitations, which has encouraged the development and increasing use of such tracers, even if the physiological properties (somewhat lower fractional myocardial tracer uptake, in particular during high coronary flow values) of both  $^{99\text{m}}\text{Tc}$ -labelled tracers are inferior to those of  $^{201}\text{Tl}$ .

### Administered activity

The usual activity is 74 MBq for stress and redistribution imaging (see Sect. “[Injected activities, dosimetry and radiation exposure](#)”). An additional 37 MBq can be given at rest for re-injection imaging if redistribution is thought to be incomplete at the time of redistribution imaging or if redistribution is predicted to be slow [8, 9]. Higher levels can be considered on an individual basis in obese patients.

### Administration

$^{201}\text{Tl}$  should be administered through a secure intravenous line in accordance with local radiation protection practices. Paravenous injection must be avoided due to risk of local tissue necrosis. If it is given through the side arm of a three-way tap through which adenosine or dobutamine is running, then it should be given over 15–30 s to avoid a bolus of the pharmacological stressor being pushed ahead of the thallium. Otherwise it can be given as a bolus injection. The thallium syringe can be flushed with either saline or glucose to ensure that the full dose is given.

*Nitrate.* Regarding nitrate administration for a rest study, cf. Sect. “[Injected activities, dosimetry and radiation exposure](#)”.

### *$^{99\text{m}}\text{Tc}$ -sestamibi and -tetrofosmin*

Two  $^{99\text{m}}\text{Tc}$ -labelled perfusion tracers are currently available commercially:  $^{99\text{m}}\text{Tc}$ -2-methoxyisobutylisonitrile (sestamibi) and  $^{99\text{m}}\text{Tc}$ -1,2-bis[bis(2-ethoxyethyl) phosphino] ethane (tetrofosmin).

$^{99\text{m}}\text{Tc}$ -sestamibi is a cationic complex which diffuses passively through the capillary and cell membrane, although less readily than  $^{201}\text{Tl}$ , resulting in lower immediate extraction. Within the cell it is localised in the mitochondria, where it is trapped [10], and retention is based on intact mitochondria, reflecting viable myocytes. Elimination of the radiotracer occurs mostly through the kidneys and the hepatobiliary system. Tetrofosmin is also cleared rapidly from the blood and its myocardial uptake is rather similar to that of sestamibi [11], with approximately 1.2% of the administered dose being taken up by the myocardium. The exact mechanism of uptake is unknown, but it is

probably similar to that of sestamibi. Elimination of the radiotracer occurs mostly through the kidneys and the hepatobiliary system, and the hepatic clearance is slightly more rapid than in the case of sestamibi [12].

For both  $^{99m}\text{Tc}$ -labelled tracers:

- Splanchnic uptake and excretion are markedly higher than for  $^{201}\text{Tl}$ , which may occasionally complicate interpretation of the inferior wall perfusion.
- The tracer molecules taken up by the cardiac myocytes remain within the cells: usually two visits on two different days are necessary to obtain optimal stress and rest images.

After intravenous injection, these  $^{99m}\text{Tc}$ -labelled radiopharmaceuticals are distributed within the myocardium according to myocardial perfusion and viability. Unlike  $^{201}\text{Tl}$ , they have little (sestamibi) or almost no redistribution (tetrofosmin) and so separate injections are required for stress and resting studies. The higher energy of  $^{99m}\text{Tc}$  generally leads to better quality images (because of less attenuation and scatter). Moreover, the short half-life of  $^{99m}\text{Tc}$  permits much higher activities to be administered, giving better counting statistics and thus allowing performance of left ventricular (LV) ECG gating or first-pass imaging, which provides additional functional information. However, the uptake of both  $^{99m}\text{Tc}$ -labelled tracers as a function of myocardial perfusion is less avid than in the case of  $^{201}\text{Tl}$ , and so defects may be less profound (Table 1).

#### Administered activity

For a 1-day protocol, the activity injected should be divided into either a third or a quarter for the first study and either two-thirds or three-quarters for the second one. For a 2-day protocol the activities injected are usually at the same level (cf. Sect. “[Injected activities, dosimetry and radiation exposure](#)”).

#### Administration

The radiopharmaceutical should be administered through a secure intravenous line in accordance with local radiation protection practices. If paravenous injection is suspected, imaging may be tried, and if sufficient activity uptake has been obtained, the examination can be performed; otherwise, the examination should be repeated whenever possible. If the radiopharmaceutical is given through the side arm of a three-way tap through which adenosine or dobutamine are running, then it should be given over 15–30 s to avoid a bolus of the pharmacological stressor being pushed ahead of the tracer. Otherwise, it can be given as a bolus injection. The syringe can be flushed with either saline or glucose to ensure that the full dose is given. As with  $^{201}\text{Tl}$ , resting injections can be given under nitrate cover; this is important when assessing myocardial via-

**Table 1.** Comparison of  $^{201}\text{Tl}$  and  $^{99m}\text{Tc}$ -labelled agents

$^{201}\text{Tl}$	$^{99m}\text{Tc}$ agents (sestamibi, tetrofosmin)
<b>Advantages</b>	
Lower liver/bowel activity	High energy and hence better image quality
No need for routine resting injection	Stress injection at remote site (e.g. emergency room)
Redistribution into myocardium of reduced resting blood supply	First-pass or ECG-gated imaging for evaluation of global and regional ventricular function
May be better for viability evaluation	Lower radiation burden to patient
Lower radiation burden to staff	
<b>Disadvantages</b>	
Low energy—vulnerable to attenuation artefacts	High splanchnic and intestinal activity
Lower count rates—functional imaging less reliable	Two injections are required when the stress study is abnormal

bility because the absence of redistribution means that viability may be underestimated in areas with reduced resting perfusion [13, 14].

Regarding nitrate administration for a rest study, cf. Sect. “[Imaging protocols](#)”.

#### Other radiotracers

$^{99m}\text{Tc}$ -*N*-NOET [bis(*N*-ethoxy, *N*-ethyl dithiocarbamate) nitride] [15] and the Q-complexes, including Q12 (furifosmin) [16], have been tested in patients but are not commercially available in Europe.

Regarding PET tracers for perfusion imaging ( $^{13}\text{N}$ -ammonia,  $^{15}\text{O}$ -water and  $^{82}\text{Rb}$ ), cf. Sect. “[Positron emission tomography \(PET\)](#)” (Table 19).

### 3. Injected activities, dosimetry and radiation exposure

The activity of radiopharmaceutical to be administered should be determined in accordance with the European Atomic Energy Community Treaty, and in particular article 31, which has been adopted by the Council of the European Union [17]. This Directive deals with health protection of individuals with respect to the dangers of ionising radiation in the context of medical exposures. According to this Directive, Member States are required to bring into force such regulations as may be necessary to comply with the Directive. One of the criteria is the designation of diagnostic reference levels (DRL) for radiopharmaceuticals; these are defined as levels of activity for groups of stan-

ard-sized patients and for broadly defined types of equipment. It is expected that these levels will not be exceeded for standard procedures.

#### *A survey on the activities administered throughout Europe for myocardial studies*

In order to enhance knowledge of current practice throughout Europe, the results of a survey of the European national recommendations are given in Table 2.

For  $^{99m}\text{Tc}$ -labelled tracers, rather large variations in the recommendations are seen from country to country, with injected activities ranging from 250 to 1,100 MBq. For a 1-day protocol, the vast majority of countries recommend 250–350 MBq for the first injection, and three times this for the second study. In a few countries this factor recommended is about 2.5. In some countries there is no information on a 1-day protocol, while in a few other countries no information is given regarding a 2-day protocol. In one country, activity is administered per kg body weight; a few other countries suggest increased activity in obese patients. In most countries, the recommendations are the same for sestamibi and tetrofosmin; small differences are seen in some countries or one of these tracers is not used or unavailable.

For  $^{201}\text{Tl}$  stress-redistribution images, nearly all recommended values are between 74 and 111 MBq, though a few countries go a little higher. For a re-injection study most countries recommend 37 MBq, while a few recommend higher activity amounts. A few countries do not provide recommendations with respect to  $^{201}\text{Tl}$ .

The recommendations from some countries show large ranges, while others give fairly narrow limits. Some of the variation may be due to the fact that the recommendations derive from different sources, e.g. some are recent national recommendations while others are published by national regulatory institutions (cf. Table 2).

#### *Activities administered: recommendations*

It is not possible to make precise recommendations in these guidelines regarding injected activities, since hard evidence documenting superior results with certain activities is not available. The injected activity is always a compromise between higher activities to obtain better image quality and lower activities to keep radiation doses as small as possible. This compromise has apparently had a problematic consequence: in order to keep the radiation dose at almost the same level for 1-day and 2-day  $^{99m}\text{Tc}$  tracer protocols, it is accepted that the average image quality will be inferior with the 1-day protocol. This appears problematic.

In general the activity needed is higher with:

- A single-head compared to a multiple-head camera system
- Gated imaging
- Shorter imaging time

- Attenuation/scatter compensation
- High body weight
- One-day  $^{99m}\text{Tc}$  protocols (compared to 2-day protocols)

It has been shown that the activity injected for a 1-day  $^{99m}\text{Tc}$  protocol at the second examination needs to be about three times higher than the first administered activity [18].

Based on widespread consensus, on our general experience that a significant number of myocardial perfusion SPECT studies are characterised by suboptimal image quality, and finally on phantom experiments [19], we recommend injection of the following activities in a normal weight adult patient for a gated study on a multiple-head camera:

$^{99m}\text{Tc}$ -sestamibi or -tetrofosmin:

- Two-day protocol: 600–900 MBq/study
- One-day protocol: 400–500 MBq for the first injection, three times more for the second injection.

$^{201}\text{Tl}$ :

- Stress redistribution: 74–111 MBq
- Re-injection: 37 MBq

In light of the European Directive and current practice throughout Europe, the above activities for  $^{99m}\text{Tc}$ -sestamibi,  $^{99m}\text{Tc}$ -tetrofosmin and  $^{201}\text{Tl}$  chloride should be considered only as a general indication, based on literature data and current experience. It should be noted, however, that in each country nuclear medicine physicians should respect the DRLs and the rules laid down by the local legislation. The injection of activities greater than local DRLs should be justified.

#### Radiation dosimetry

The absorbed radiation doses to various organs in healthy subjects following administration of  $^{99m}\text{Tc}$ -sestamibi,  $^{99m}\text{Tc}$ -tetrofosmin and  $^{201}\text{Tl}$  chloride are given in Table 3. The data are quoted from ICRP [20].

The small variations for rest and stress studies are not clinically significant. The effective doses in the last column are calculated according to the ICRP recommendations [22], by taking into account organ and radiation weighting factors. For paediatric patients, additional values for absorbed dose per unit activity administered (mGy/MBq) are given in one of the ICRP reports [20].

The activities to be administered for paediatric patients should be modified according to the recommendations of the Paediatric Task Group of the EANM [23].

#### Organs at risk

The organs with the highest absorbed dose per unit activity administered (mGy/MBq) are the gall-bladder and kidneys for  $^{99m}\text{Tc}$ -sestamibi, the gall-bladder and colon for  $^{99m}\text{Tc}$ -

**Table 2.** Recommendations made by national European regulatory authorities, national societies and other sources with respect to injected activities (in MBq) for <sup>99m</sup>Tc-labelled tracers (A) and for <sup>201</sup>Tl (B) for adults of normal weight (values may overlap over two columns)

A. <sup>99m</sup> Tc-labelled tracers			
2-Day protocol: activity injected per image acquisition			
<500 MBq	500–750 MBq	750–1,000 MBq	No information available/not used
Germany <sup>a</sup> , Hungary <sup>b</sup> , Switzerland <sup>c</sup> , UK <sup>d</sup> , Finland <sup>e</sup>	Bulgaria <sup>f</sup> , Croatia <sup>g</sup> , Denmark <sup>h</sup> , Italy <sup>i</sup> , Luxembourg <sup>j</sup> , Poland <sup>k</sup> , Romania <sup>l</sup> , Slovenia <sup>m</sup> , Sweden <sup>n</sup> , The Netherlands <sup>o</sup>	Austria <sup>p</sup> , Belgium <sup>q</sup> , Czech Republic <sup>r</sup> , France <sup>s</sup> , Israel <sup>t</sup> , Portugal <sup>u</sup> , Spain <sup>v</sup> , Turkey <sup>w</sup>	Bosnia, Cyprus <sup>z</sup> , Estonia, Greece <sup>x</sup> , Ireland, Latvia, Lithuania, Norway, Russia, Serbia Montenegro <sup>y</sup>
1-Day protocol: activity injected for first image acquisition			
250–350 MBq		>350 MBq	No information available/not used
Austria <sup>p</sup> , Belgium <sup>q</sup> , Bulgaria <sup>f</sup> , Cyprus <sup>z</sup> , Czech Republic <sup>r</sup> , Estonia, Finland <sup>e</sup> , France <sup>s</sup> , Germany <sup>a</sup> , Greece <sup>x</sup> , Hungary <sup>b</sup> , Israel <sup>t</sup> , Latvia, Luxembourg <sup>j</sup> , Portugal <sup>u</sup> , Switzerland <sup>c</sup> , The Netherlands <sup>o</sup> , UK <sup>d</sup>		Denmark <sup>h</sup> , Italy <sup>i</sup> , Poland <sup>k</sup> , Romania <sup>l</sup> , Spain <sup>v</sup> , Sweden <sup>n</sup> , Turkey <sup>w</sup>	Bosnia, Croatia <sup>g</sup> , Ireland, Lithuania, Norway, Russia, Serbia Montenegro <sup>y</sup> , Slovak Republic, Slovenia <sup>m</sup>
1-Day protocol: factor increase of activity from first to second injection			
ca. 2.5	ca. 3		No information available/not used
Estonia, Germany <sup>a</sup> , Greece <sup>x</sup> , Latvia, Romania <sup>l</sup> , Spain <sup>v</sup> , Switzerland <sup>c</sup> , The Netherlands <sup>o</sup>	Austria <sup>p</sup> , Belgium <sup>q</sup> , Bulgaria <sup>f</sup> , Cyprus <sup>z</sup> , Czech Republic <sup>r</sup> , Denmark <sup>h</sup> , Finland <sup>e</sup> , France <sup>s</sup> , Hungary <sup>b</sup> , Israel <sup>t</sup> , Italy <sup>i</sup> , Luxembourg <sup>j</sup> , Poland <sup>k</sup> , Portugal <sup>u</sup> , Sweden <sup>n</sup> , Turkey <sup>w</sup> , UK <sup>d</sup>		Bosnia, Croatia <sup>g</sup> , Ireland, Lithuania, Norway, Russia, Serbia Montenegro <sup>y</sup> , Slovak Republic, Slovenia <sup>m</sup>
B. <sup>201</sup> Tl			
Stress redistribution: activity injected per study			
74 MBq	>74 MBq		No information available/not used
Bulgaria <sup>f</sup> , Poland <sup>k</sup>	Austria <sup>p</sup> , Belgium <sup>q</sup> , Croatia <sup>g</sup> , Cyprus <sup>z</sup> , Czech Republic <sup>r</sup> , Denmark <sup>h</sup> , Estonia, Finland <sup>e</sup> , France <sup>s</sup> , Germany <sup>a</sup> , Greece <sup>x</sup> , Hungary <sup>b</sup> , Israel <sup>t</sup> , Italy <sup>i</sup> , Luxembourg <sup>j</sup> , Portugal <sup>u</sup> , Romania <sup>l</sup> , Serbia Montenegro <sup>y</sup> , Slovenia <sup>m</sup> , Spain <sup>v</sup> , Switzerland <sup>c</sup> , Sweden <sup>n</sup> , The Netherlands <sup>o</sup> , Turkey <sup>w</sup> , UK <sup>d</sup>		Bosnia, Norway, Ireland, Latvia, Lithuania, Russia, Slovak Republic

<sup>a</sup>German Reference Activities, Bundesamt für Strahlenschutz, 2003<sup>b</sup>National Board of Nuclear Medicine, 2003<sup>c</sup>Dept. of Nucl. Med. and Div. of Cardiology, University Hospital Basel, 2003<sup>d</sup>ARSAC Notes for Guidance, DRL and BNMS, BNCS, BCS Guidelines. *Nucl Med Commun* 2000;21: suppl.<sup>e</sup>Radiation and Nuclear Safety Authority of Finland (STUK), 2004<sup>f</sup>Clinical Centre of Nuclear Medicine Radiotherapeutics, Medical University, Sofia, 2004<sup>g</sup>National Regulatory Authorities<sup>h</sup>Recommendations of the Danish Society of Clinical Physiology and Nuclear Medicine, 1999<sup>i</sup>Ministry of Health (DL 187/2000)<sup>j</sup>Ste Thérèse (Ministry of Health)<sup>k</sup>Polish Society of Nuclear Medicine<sup>l</sup>Basic Rules for Radiologic Safety National Regulatory Safety Committee (CNCAN). Romanian Society of Nuclear Medicine, 2004<sup>m</sup>University of Medical Centre, Nuclear Medicine, Ljubljana, 2003, proposed guidelines, unpublished<sup>n</sup>SSI FS 2002:1, Sakbeteckning 7 (Swedish Radiation Protection Authority)<sup>o</sup>Diakonessenhuis Utrecht, 2003<sup>p</sup>Recommendations of Austrian Society of Nuclear Medicine ÖGN (Institution), 2004<sup>q</sup>Belgian Society of Nuclear Medicine, 2000<sup>r</sup>Nuclear cardiology in the Czech Republic in 2001, *Cor Vasa* 2003;45:50–3<sup>s</sup>Recommendations from Working Group on Nuclear Cardiology, published in *Arch Mal Coeur Vaiss*, 2003 Jun;96(6):695–711<sup>t</sup>Nuclear Cardiology and Nuclear Medicine, Rabin Med. Centre, 2003<sup>u</sup>Survey from 15 Portuguese institutions, 2003<sup>v</sup>Task Group on Nuclear Cardiology (Spanish Society of Nuclear Medicine)<sup>w</sup>Turkish Society of Nuclear Medicine—Cardiology Task Group; Nuclear Cardiology Guidelines, 2001; 10S 41–56, *Turk J Nucl Med*<sup>x</sup>University of Patras, Nuclear Medicine Department, 2003<sup>y</sup>Inst. Nucl. Med., Clinical Centre of Serbia, Belgrade, 2004<sup>z</sup>No national guidelines. Activities used in 2003 in Nicosia General Hospital are shown

**Table 3.** Absorbed doses

	Absorbed dose per unit activity administered (mGy/MBq) for adults					
	mGy/MBq			mGy/patient examination <sup>a</sup>		
	<sup>99m</sup> Tc		<sup>201</sup> Tl chloride	<sup>99m</sup> Tc		<sup>201</sup> Tl chloride
	Sestamibi <sup>b</sup>	Tetrofosmin <sup>b</sup>		Sestamibi	Tetrofosmin	
Bone surfaces	0.01	0.01	0.34	10	10	27
Gall-bladder	0.04 (0.03)	0.04 (0.03)	0.07	40	30	6
Small intestine	0.01	0.01	0.14	10	10	11
Colon	0.02	0.02	0.23	20	20	18
Kidneys	0.04 (0.03)	0.01	0.48	30	10	38
Urinary bladder	0.01	0.02 (0.03)	0.04	10	20	3
Heart	0.006 (0.007)	0.004 (0.005)	0.20	6	5	16
Ovaries	0.009 (0.008)	0.008	0.73	9	8	58
Testes	0.004	0.002 (0.003)	0.45	40	30	36
Effective dose <sup>c</sup>	0.0082 (mSv/MBq)	0.0073 (mSv/MBq)	0.22 (mSv/MBq)	8.1 mSv	7.2 mSv	17.6 mSv

The absorbed doses (mGy/MBq) are adopted from [20, 21]. The absorbed doses for <sup>99m</sup>Tc-labelled tracers are average doses for rest and stress studies. The effective doses are calculated according to the recommendations given by [22].

<sup>a</sup>The absorbed doses per patient examination are calculated with an average amount of activity for <sup>99m</sup>Tc-labelled tracers of 2×500 MBq (for a 2-day protocol) and for <sup>201</sup>Tl chloride as a single-injection examination of 80 MBq. The dose will increase with re-injection of <sup>201</sup>Tl chloride and with a 1-day <sup>99m</sup>Tc protocol, according to the increased activity administered, and it will be reduced correspondingly if only a single <sup>99m</sup>Tc study is performed.

<sup>b</sup>Data in brackets are values that are valid for stress studies. These values are only given when dose coefficients differed between rest and stress.

<sup>c</sup>It should be noted that the entity “Effective dose” does not necessarily reflect the radiation risk associated with this nuclear medicine examination. The effective dose values given in these guidelines are used to compare the exposure due to different nuclear medicine procedures. If the risk associated with the procedure is to be assessed, it is mandatory to adjust the radiation-associated risk factors at least according to the gender and age distribution of the institution’s patient population.

tetrofosmin and the ovaries, bone surface and kidney for <sup>201</sup>Tl chloride. The exposure of a number of other organs is shown in Table 3.

#### *Positron-emitting radioactive tracers for myocardial perfusion imaging*

The effective doses for PET tracers used in cardiology are:

- <sup>18</sup>F-FDG: 0.019 mSv/MBq
- <sup>13</sup>N-ammonia: 0.002 mSv/MBq
- <sup>18</sup>O-water: 0.00093 mSv/MBq
- <sup>82</sup>Ru: 0.0034 mSv/MBq

*Activities administered.* National recommendations are generally not available. Activities commonly used are shown in Table 19 in Sect. “Positron emission tomography (PET)”.

#### *Radiation exposure levels to the hospital staff and to relatives of patients*

In general, radiation exposure to relatives is limited, and no special precautions are needed for studies with either

<sup>99m</sup>Tc-labelled tracers or <sup>201</sup>Tl chloride. One-day protocols for patients taking care of infants should be avoided. It should be noted that for the injected patient the absorbed dose is lower with <sup>99m</sup>Tc-labelled tracers than with <sup>201</sup>Tl chloride, but that the radiation exposure to the surroundings is lower with <sup>201</sup>Tl chloride than with <sup>99m</sup>Tc-labelled tracers (cf. Tables 3 and 4).

The German Radiation Protection Board (SSK) [24] assessed, in a “worst case scenario”, the radiation exposure to the staff of a general hospital outside the nuclear medicine or nuclear cardiology department. In addition, the exposure of relatives was calculated. The results of these assessments can be found in Table 4. The data given in Table 4 do not represent the exposure of staff performing the actual myocardial studies in a nuclear medicine or cardiology department.

#### *Pregnancy and lactation*

##### *Pregnancy*

According to the “Guidance for protection of unborn children and infants irradiated due to parental medical exposures” published on-line by the European Commission [25], if pregnancy is confirmed, or if the woman is to be

**Table 4.** Exposure levels to staff outside nuclear medicine departments and to relatives after myocardial perfusion imaging

	$^{201}\text{Tl}$ chloride	$^{99\text{m}}\text{Tc}$ -sestamibi/ tetrofosmin
<i>Personnel</i>		
Nurses working at a general ward outside nuclear medicine or nuclear cardiology	480 $\mu\text{Sv}/\text{year}$	580 $\mu\text{Sv}/\text{year}$
Intensive care unit staff	37 $\mu\text{Sv}/\text{year}$	73 $\mu\text{Sv}/\text{year}$
<i>Doctors</i>		
General ward	13 $\mu\text{Sv}/\text{year}$	110 $\mu\text{Sv}/\text{year}$
Special functions	100 $\mu\text{Sv}/\text{year}$	1,100 $\mu\text{Sv}/\text{year}$
Technologists outside nuclear medicine or nuclear cardiology	25 $\mu\text{Sv}/\text{year}$	220 $\mu\text{Sv}/\text{year}$
Transport	38 $\mu\text{Sv}/\text{year}$	170 $\mu\text{Sv}/\text{year}$
<i>Relatives or "helpers"</i>		
In the hospital	1 $\mu\text{Sv}/\text{patient}$	8.3 $\mu\text{Sv}/\text{patient}$
At home	1.9 $\mu\text{Sv}/\text{patient}$	8.3 $\mu\text{Sv}/\text{patient}$
Child with NM procedure—parent	60 $\mu\text{Sv}/\text{patient}$	12 $\mu\text{Sv}/\text{patient}$
Parent with NM procedure—child	150 $\mu\text{Sv}/\text{patient}$	93 $\mu\text{Sv}/\text{patient}$
Other patients in the hospital	42 $\mu\text{Sv}/\text{patient}$	300 $\mu\text{Sv}/\text{patient}$

The values in Table 3 suggest that the 1 mSv/year threshold is never exceeded. This holds true for professionals in contact with the patients and for relatives in contact with the patient outside the hospital. It should be noted that the exposure levels given above do not show the total exposure for a member of the technical staff who may take care of several patients a day. In the case of, for example, echocardiographic examinations of injected patients, a cardiological nuclear medicine physician may run the risk of exceeding the 1-mSv/year limit

treated as pregnant, one of the three following approaches is recommended:

- The use of other diagnostic methods
- Postponement of the nuclear medicine examination until after delivery, if this is considered to be clinically acceptable

- Performance of the examination with special attention to the radiation dose to the unborn child—applicable in cases in which a delay is not medically acceptable.

It must be stressed that the above approaches are examples as to what measures may be appropriate; there might be others. Possible means for dose reduction include careful selection of the radiopharmaceutical and radionuclide to minimise the dose to the unborn child.

#### Lactation

According to the European Commission guidelines [25], interruption of breast-feeding is not essential for  $^{201}\text{Tl}$  chloride up to 80 MBq and not at all for  $^{99\text{m}}\text{Tc}$ -labelled radionuclides. Close contact with infants should be restricted during this period, in particular when  $^{99\text{m}}\text{Tc}$ -labelled tracers are used.

If breast-feeding is to be continued after a  $^{201}\text{Tl}$  procedure with an injected activity >80 MBq, it is recommended that breast milk be expressed some days beforehand, so that it can be stored for use by the child after administration of the radiopharmaceutical. Once the radiopharmaceutical has been administered, the first breast milk should be expressed and discarded. Consideration should be given to whether a study with a  $^{99\text{m}}\text{Tc}$ -labelled tracer could be done instead.

## 4. Stress tests

### Stress testing procedures, general overview

Dynamic exercise is the technique of choice in the assessment of patients with suspected or known coronary artery disease provided that the patient is able to exercise to an acceptable work load (Fig. 1; Table 5). In addition, information about exercise tolerance is obtained. However, it should not be performed in patients who cannot achieve an adequate haemodynamic response because of non-cardiac physical limitations such as pulmonary, peripheral vascular or musculoskeletal abnormalities or because of poor motivation. These patients, as well as those who are unable to exercise at all for non-cardiac reasons (e.g. owing to severe pulmonary disease, arthritis, amputation or neuro-

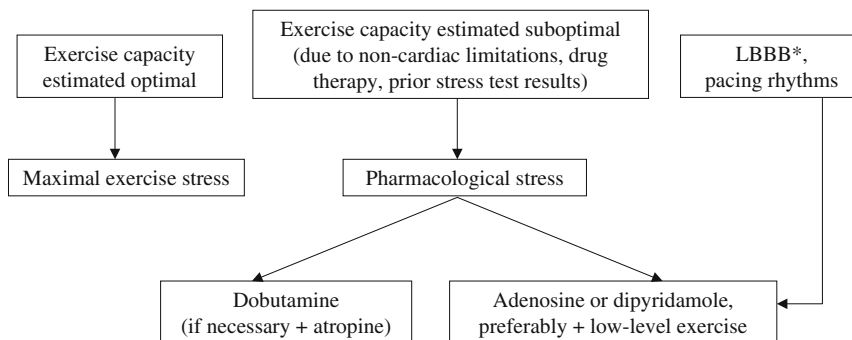


**Fig. 1.** Selection of stress modality\*. *LBBB* Left bundle branch block

**Table 5.** Stress types used in relation to myocardial perfusion imaging

Exercise stress		Bicycle stress Treadmill stress
Pharmacological stress	Vasodilator agents	Adenosine Dipyridamole “Hybrid tests”: both can be combined with low-level exercise
	Sympathomimetic agent	Dobutamine + atropine if necessary

logical disease), should undergo pharmacological stress perfusion imaging, a very good alternative to dynamic exercise. Two groups of drugs are commonly used as substitutes for exercise stress testing: vasodilators (dipyridamole and adenosine), creating coronary hyperaemia, and the sympathomimetic agents (dobutamine), increasing myocardial oxygen demand.

A secure intravenous line should be established for the administration of the radiopharmaceutical during stress. Patients undergoing exercise stress should wear suitable clothing and shoes.

All stress procedures must be supervised by a qualified health care professional. Stress testing should be supervised by an appropriately trained health-care professional who may be a physician, a nurse or a technician [26]. Non-medical stressors should operate according to a locally approved procedure and may commonly work under the direct or indirect supervision of a physician. The stressor should be experienced in the selection of the most appropriate form of stress for the clinical question being asked and should have the clinical skills to recognise patients with an increased risk of complications. Appropriate facilities for cardiopulmonary resuscitation must be available and the stressor should have up-to-date knowledge of advanced life support (ALS) techniques or intermediate life support and have immediate access to personnel with ALS expertise [26].

#### Preparations before a stress study:

- The clinical history should be obtained, including the indication for the test, symptoms, risk factors, medication and prior diagnostic or therapeutic procedures.
- In diabetic patients, diet and insulin dosing should be optimised on the day of examination.
- The patient should be haemodynamically and clinically stable for a minimum of 48 h prior to the test.
- Cardiac medications which may interfere with the stress test should, if possible, be interrupted (cf. Table 6). In general, the decision on whether to interrupt drug administration should be left to the referring physician, and such interruption should ideally last for five half-lives of the drug.
- Caffeine-containing beverages (coffee, tea, cola etc.), foods (chocolate etc.) and medications (some pain relievers, stimulants and weight-control drugs) and methylxanthine-containing medications should be avoided

for at least 12 h prior to stress testing owing to interference with vasodilator tests (cf. below); this is necessary in order not to rule out any of the stress modalities.

#### Exercise stress testing procedure

##### Indications

This document will not review the indications, contraindications or diagnostic criteria for exercise stress tests,

**Table 6.** Drug and food/beverage interruption before stress test perfusion imaging

Drugs, food intake etc.	Type of stress test		
	Exercise	Vasodilator (adenosine, dipyridamole, hybrid tests)	Dobutamine ( $\pm$ atropine)
Nitrates	+	+	+
$\beta$ -Blockers	+	(+) <sup>a</sup>	+
Calcium antagonists	+	(+)	(+)
Methylxanthine-containing beverages, food and drugs	–	+	–
Persantine	+	+	–
Caffeine-containing foods and beverages	–	+	–
Fasting	–	–	–
Insulin	Check blood glucose before exercise to avoid hypoglycaemia	–	–

+ Must be interrupted, – can be continued, (+) interruption recommended by some, but evidence for improved stress test after interruption is limited or not obvious

<sup>a</sup> Extent and severity of stress defects may be underestimated [28]

since these matters are covered by other specific guidelines [27, 28]. Although exercise testing is generally a safe procedure, both myocardial infarction and death have been reported and can be expected to occur at a rate of about 1 per 10,000 tests, depending on the local case mix. Good clinical judgment should therefore be used in deciding which patients should undergo exercise testing.

The electrocardiogram, heart rate and blood pressure should be monitored and recorded during each stage of exercise as well as during ST segment abnormalities and chest pain. The patient should be continuously monitored for transient rhythm disturbances, ST segment changes and other electrocardiographic manifestations of myocardial ischaemia. Monitoring of a single ECG lead during stress testing is not sufficient for the detection and recognition of arrhythmias or ischaemic patterns. Nine or 12 leads are recommended.

#### Equipment and protocols

Both treadmill and bicycle ergometers are used for exercise testing. Although the bicycle ergometer is generally smaller and less expensive than the treadmill and produces less motion of the upper body, quadriceps fatigue in patients who are not experienced cyclists is a limitation because subjects usually stop before reaching their maximum oxygen uptake. Several treadmill exercise protocols are available, differing in speed and inclination of the treadmill; the Bruce and modified Bruce protocols are the most widely used. Supine or semi-supine exercise is not ideal and should be reserved for exercise radionuclide angiocardigraphy.

Contraindications (absolute) to maximal, dynamic exercise are:

- Acute coronary syndrome, until the patient has been stable for at least 24 h and the risk is clinically assessed as acceptable
- Acute pulmonary embolism
- Uncontrolled, severe hypertension (blood pressure  $\geq 200/110$  mmHg)
- Severe pulmonary hypertension
- Acute aortic dissection
- Symptomatic aortic stenosis and hypertrophic, obstructive cardiomyopathy
- Uncontrolled cardiac arrhythmias causing symptoms or haemodynamic instability

Contraindications (relative) to maximal, dynamic exercise are:

- Patients with decompensated or inadequately controlled congestive heart failure
- Active deep vein thrombophlebitis or deep vein thrombosis
- Acute endocarditis, myocarditis, pericarditis
- Left bundle branch block, ventricular paced rhythm

A maximal exercise test should adhere to the following steps:

- Before exercise an intravenous (i.v.) cannula should be inserted for radiopharmaceutical injection.
- The electrocardiogram should be monitored continuously during the exercise test and for at least 3–5 min of recovery. A 12-lead electrocardiogram should be obtained at every stage of exercise, at peak exercise and during recovery.
- The blood pressure should be checked at least every 3 min during exercise.
- Exercise should be symptom limited, with patients achieving  $\geq 85\%$  of their age-predicted maximum heart rate (maximal age – predicted heart rate =  $220 - \text{age}$ ).
- The radiopharmaceutical should be injected close to the peak exercise. The patients should be encouraged to continue the exercise for at least 1 min after the tracer injection.

An exercise test sometimes has to be terminated before maximal age-predicted heart rate has been achieved.

Absolute indications for early termination of exercise are:

- Marked ST segment depression ( $\geq 3$  mm)
- Ischaemic ST segment elevation of  $>1$  mm in leads without pathological Q waves
- Appearance of ventricular tachyarrhythmia [the occurrence of supraventricular tachycardia or atrial fibrillation with a high heart rate response is an indication to terminate exercise]
- A decrease in systolic blood pressure of  $>20$  mmHg, despite increasing work load, when accompanied by other evidence of ischaemia
- Markedly abnormal elevation of blood pressure (systolic blood pressure  $\geq 250$  mm or diastolic blood pressure  $\geq 130$  mmHg)
- Angina sufficient to cause distress to the patient
- Central nervous system symptoms (e.g. ataxia, dizziness or near-syncope)
- Peripheral hypoperfusion (cyanosis or pallor)
- Sustained ventricular tachycardia or fibrillation
- Inability of the patient to continue the test
- Technical difficulties in monitoring ECG or blood pressure

Relative indications for early termination of exercise are:

- ST segment depression  $>2$  mm horizontal or downsloping
- Arrhythmias other than sustained ventricular tachycardia [including multifocal premature ventricular contractions (PVCs), triplets of PVCs, supraventricular tachycardia, heart block or bradyarrhythmias], especially if symptomatic
- Fatigue, dyspnoea, cramp or claudication
- Development of bundle branch block or intraventricular conduction defect that cannot be distinguished from ventricular tachycardia

## Adenosine/dipyridamole stress tests

### Mechanism of action

Adenosine is a direct coronary arteriolar dilator and in a normal coronary artery results in a three- to fourfold increase in myocardial blood flow. Dipyridamole is an indirect coronary arteriolar dilator that increases the tissue levels of adenosine by preventing the intracellular re-uptake and deamination of adenosine. Adenosine and dipyridamole result in a modest increase in heart rate and a modest decrease in both systolic and diastolic blood pressures.

Myocardium supplied by a diseased coronary artery has a reduced perfusion reserve and this leads to heterogeneity of perfusion during vasodilation or even to myocardial ischaemia caused by coronary steal. Because myocardial tracer uptake is proportional to perfusion, this results in heterogeneous uptake of tracer.

Caffeine-containing beverages (coffee, tea, cola, etc.), foods (chocolate, etc.) and medications (some pain relievers, stimulants and weight control drugs) and methylxanthine-containing medications that antagonise adenosine should be discontinued at least 12 h before adenosine or dipyridamole stress (or longer for long-acting methylxanthine preparations). Persantine should be interrupted for at least 24 h (cf. Table 6). Pentoxifylline and clopidogrel need not be stopped prior to adenosine stress perfusion imaging.

### Indications

The indications are the same as for exercise myocardial perfusion imaging in patients not expected to be able to achieve maximal, age-predicted heart rate during exercise. Adenosine or dipyridamole (without exercise) should be preferred to exercise in cases of left bundle branch block (cf. Fig. 1).

Absolute contraindications to vasodilator stress tests are:

- Acute coronary syndrome (vasodilator stress test may be considered when the patient has been stable for at least 24 h and the clinically assessed risk is deemed acceptable)
- Severe bronchospasm

- Greater than first-degree heart block or sick sinus syndrome, without a pacemaker
- Symptomatic aortic stenosis and hypertrophic obstructive cardiomyopathy
- Systolic blood pressure <90 mmHg
- Unstable angina
- Cerebral ischaemia

Relative contraindications to vasodilator stress tests are:

- Severe sinus bradycardia (heart rate <40/min)
- Severe atherosclerotic lesions of extracranial artery
- Use of dipyridamole during the last 24 h (this point is included in several guidelines on dipyridamole stress testing, to avoid possible enhancement of the drug effect).

### Procedure

An infusion or a syringe pump is necessary for adenosine administration at a constant infusion rate. An i.v. line with a dual-port Y-connector is required to allow tracer injection without interruption of the adenosine infusion.

Dipyridamole can be administered by hand injection. This obviates the need for a Y connector.

Electrocardiographic (ECG) and blood pressure monitoring should be carried out as with exercise stress testing (Fig. 2).

### Combination with low-level exercise

Low-level exercise is performed routinely in many laboratories in conjunction with vasodilator tests. Low-level exercise significantly reduces the side-effects (flushing, dizziness, nausea, headache, vasodilator-induced hypotension) and improves image quality due to lower bowel activity. Accordingly, if possible low-level exercise is recommended in combination with vasodilator stress [29–31]. Low-level exercise is not recommended for patients with left bundle branch block or ventricular paced rhythm (Fig. 1).

**Adenosine dose.** Adenosine should be given as a continuous infusion at 140 µg/kg/min over 4–6 min with

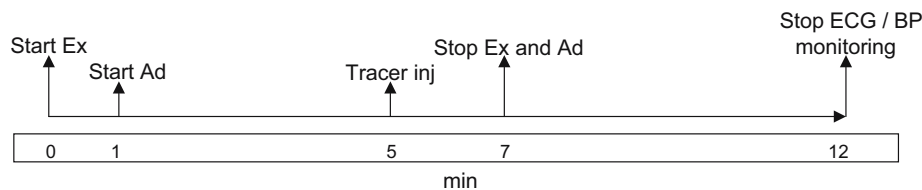


**Fig. 2.** Adenosine low-level exercise flow chart (“hybrid test”). Flow chart example for combined low-level exercise (*Ex*) and vasodilator infusion (“hybrid test”), shown here as the protocol frequently used: brief warm-up exercise (e.g. 1 min), start of adenosine (*Ad*) infusion for (4–)6 min during continued, stable exercise. After 4 (2–4) min of

adenosine infusion, the tracer is injected during continued adenosine infusion (for  $^{201}\text{Tl}$  at least 1 min, for  $^{99\text{m}}\text{Tc}$  tracers preferably 2 min). Monitoring may be interrupted when heart rate and blood pressure are back to baseline and the patient is free of symptoms. For early termination of vasodilator test, see text

injection of the tracer at 3–4 min. The infusion should be continued for 1–2 min after tracer injection. For patients at risk of complications (recent ischaemic event, borderline hypotension, inadequately controlled asthma), the infusion can be started at a lower dose (50 µg/kg/min). If this dose is tolerated for 1 min, the rate can be increased to 75, 100 and 140 µg/kg/min at 1-min intervals and then continued for 4 min. The tracer should be injected 1 min after starting the 140-µg/kg/min dose. A shorter duration of infusion may also be effective [32].

*Dipyridamole dose.* Dipyridamole should be given as a continuous infusion intravenously at 140 µg/kg/min over 4 min. The tracer is injected 3–5 min after the completion of dipyridamole infusion.

#### Early termination of vasodilator stress test

Infusion of adenosine or dipyridamole should be stopped early under the following circumstances:

- Severe hypotension (systolic blood pressure <80 mmHg)
- Persistent second-degree or sign of third-degree atrioventricular or sino-atrial block
- Wheezing
- Severe chest pain

#### Side-effects

*Adenosine.* Minor side-effects are common and occur in approximately 80% of patients. The common side-effects are flushing (35–40%), chest pain (25–30%), dyspnoea (20%), dizziness (7%), nausea (5%) and symptomatic hypotension (5%). Chest pain is non-specific and does not necessarily indicate myocardial ischaemia. High-degree atrioventricular (AV) and sino-atrial (SA) block occurs in approximately 7% of cases. ST segment depression  $\geq 1$  mm occurs in 15–20% of cases. However, unlike chest pain, this is indicative of myocardial ischaemia. Fatal or non-fatal myocardial infarction is rare, the reported incidence being less than 1 in 1,000 cases.

Because of the very short half-life of adenosine (<10 s), most side-effects resolve rapidly on discontinuing the infusion. Aminophylline is only rarely required [33].

*Dipyridamole.* More than 50% of patients develop side-effects (flushing, chest pain, headache, dizziness or hypotension). The frequency of these side-effects is less than that seen with adenosine, but they last longer (15–25 min) and aminophylline (125–250 mg, i.v.) may be required, preferably not earlier than 3 min after tracer injection. The incidence of high-degree AV and SA block with dipyridamole is less than that observed with adenosine (2%) [34].

#### Dobutamine stress test

##### Mechanism of action

Dobutamine results in a dose-related increase in myocardial oxygen demand due to increase in heart rate and blood pressure and usually also in myocardial contractility (in severe ischaemic heart disease, contractility may be reduced with high doses of dobutamine). Due to these effects, it causes secondary coronary vasodilation and hence increased coronary oxygen supply similar to exercise stress. In areas supplied by significantly stenosed coronary arteries, the increase in flow is blunted, i.e. the flow reserve is reduced.

##### Dobutamine dose

Dobutamine is infused incrementally, starting at a dose of (5 to) 10 µg/kg/min and increasing at 3-min intervals to 20, 30 and 40 µg/kg/min. It is customary to use atropine in patients if heart rate does not reach 85% of age-predicted maximal heart rate.

##### Indications

Dobutamine is a secondary pharmacological stressor that is used in patients who cannot undergo exercise stress and have contraindications to vasodilator stressors. Common contraindications to the execution of a dobutamine stress test are indicated below.

##### Contraindications to dobutamine stress test:

- The same as for dynamic exercise, cf. above
- Patients on  $\beta$ -blockers may not show an adequate heart rate response to dobutamine (relative contraindication)

##### Contraindications to atropine administration:

- Narrow angle glaucoma
- Obstructive uropathy, including bladder neck obstruction from prostatic hypertrophy
- Atrial fibrillation with an uncontrolled heart rate
- Obstructive gastrointestinal disease or paralytic ileus
- Prior adverse reaction to administration
- Patients should be informed of possible difficulties while driving in the 2 h following atropine administration due to reduced ocular accommodation

##### Procedure

An infusion pump is necessary for dobutamine administration. An i.v. line with a Y-connector is required for

injection of radioisotope during dobutamine infusion. ECG monitoring and blood pressure monitoring should be performed as with other pharmacological stressors.

Dobutamine infusion should start at a dose of (5–)10  $\mu\text{g}/\text{kg}/\text{min}$ . The dobutamine dose should then be increased at 3-min intervals up to a maximum of 40  $\mu\text{g}/\text{kg}/\text{min}$ . The radiotracer should be injected when the heart rate is  $\geq 85\%$  of the age-predicted maximum heart rate (maximal age – predicted heart rate =  $220 - \text{age}$ ). Dobutamine infusion should be continued for 2 min after the radiotracer injection.

Atropine could be given in the presence of submaximal heart rate response (0.25 mg, i.v., one to three times with 1/2-min intervals) [35] (Fig. 3).

### Early termination of dobutamine

The indications for early termination of dobutamine are similar to those for exercise stress. Termination due to ventricular tachycardia or ST segment elevation is more likely with dobutamine than with other stressors.

### Side-effects

Dobutamine has a relatively rapid onset and cessation of action (plasma half-life of 120 s), allowing easy control of its effects. Side-effects occur in about 75% of patients. The common side-effects are palpitation (29%), chest pain (31%), headache (14%), flushing (14%), dyspnoea (14%) and significant supraventricular or ventricular arrhythmias (8–10%). Ischaemic ST segment depression occurs in approximately one-third of patients undergoing dobutamine infusion. Severe side-effects may require i.v. administration of a  $\beta$ -blocker such as esmolol, sotalol or propranolol. Hypotension can also occur during dobutamine infusion and is not usually a marker of severe ischaemia or severe LV dysfunction.

## 5. Imaging protocols

$^{201}\text{Tl}$  protocols are described first, followed by  $^{99\text{m}}\text{Tc}$  tracer protocols and finally dual-isotope protocols. PET tracer protocols are described in Sect. “Positron emission tomography”.

A summary of the drawbacks of different SPECT imaging protocols is given in Table 7.

### Thallium-201

After an i.v. injection of  $^{201}\text{Tl}$  at stress, the radiotracer is distributed in the myocardium according to myocardial perfusion and viability.  $^{201}\text{Tl}$  subsequently redistributes from its initial distribution over several hours, thus allowing redistribution images which reflect baseline perfusion and viability to be acquired usually 3–4 h later. Comparison between the stress and redistribution images distinguishes between the reversible defect of inducible hypoperfusion and the fixed defect of myocardial necrosis, although in some cases redistribution may be incomplete at 4 h. A second injection of  $^{201}\text{Tl}$  can then be given and re-injection images acquired for a more accurate assessment of myocardial viability [8].

Different imaging protocols can be followed, depending on clinical indication(s) and local practices: stress redistribution, stress re-injection, stress redistribution–re-injection or stress re-injection–delayed 24-h imaging [36]:

*Stress imaging.* should begin within 5–10 min of tracer injection and should be completed within 30 min of injection.

*Redistribution imaging.* should be performed after 3–4 h of rest.

*Re-injection.* In patients with severe perfusion defects in the stress images or if redistribution is thought to be

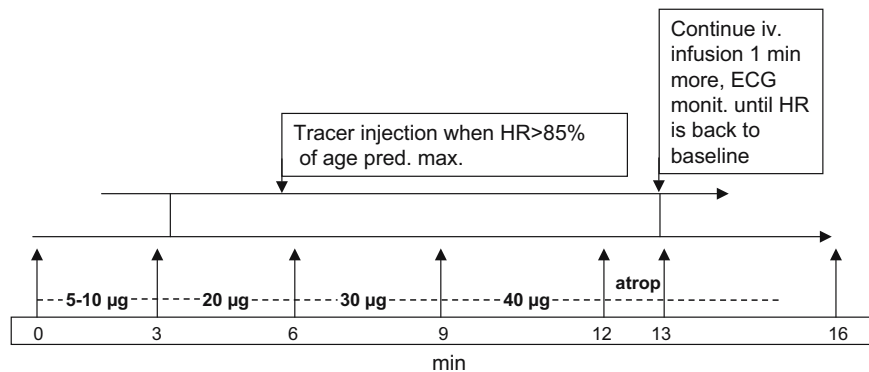


**Fig. 3.** Dobutamine flow chart. Dobutamine is infused intravenously in increasing dosages until the heart rate (HR) is  $\geq 85\%$  of the predicted maximum value, from 5 or 10  $\mu\text{g}/\text{kg}/\text{min}$  up to max. 40  $\mu\text{g}/\text{kg}/\text{min}$ . If the desired heart rate is not attained with the latter dosage, atropine (atrop) may be added during continued dobutamine

infusion. Tracer is injected at  $\geq 85\%$  maximal heart rate, which should be maintained for 1 min after tracer injection. For early termination of dobutamine test, see text. Monitoring is continued until heart rate has returned to baseline

**Table 7.** Disadvantages associated with different imaging protocols

Protocol	Disadvantages
$^{201}\text{Tl}$ stress—4-h redistribution	Attenuation artefacts may complicate evaluation of tracer distribution Evaluation of LVEF and wall motion is inferior compared with $^{99\text{m}}\text{Tc}$ -labelled tracers
$^{99\text{m}}\text{Tc}$ -sestamibi or $^{99\text{m}}\text{Tc}$ -tetrofosmin, general	Radiation dose to patient higher than with $^{99\text{m}}\text{Tc}$ Tracer uptake often (rest and pharmacological stress studies) high in subdiaphragmatic regions with extracardiac hot spots
$^{99\text{m}}\text{Tc}$ -sestamibi or $^{99\text{m}}\text{Tc}$ -tetrofosmin 2-day stress/rest protocol	Logistics: patient must come on two different days if stress study is not normal
$^{99\text{m}}\text{Tc}$ -sestamibi or $^{99\text{m}}\text{Tc}$ -tetrofosmin 1-day stress/rest protocol	Reversibility may be underestimated because of interference from remaining myocardial activity from the stress study
$^{99\text{m}}\text{Tc}$ -sestamibi or $^{99\text{m}}\text{Tc}$ -tetrofosmin 1-day rest/stress protocol	Two tracer injections necessary even if stress study is normal Stress defects may be less clearly visualised due to interference from remaining myocardial activity from the resting study
Dual-isotope protocol	Comparison of $^{201}\text{Tl}$ and $^{99\text{m}}\text{Tc}$ tracer uptake may be influenced by differences in attenuation and spill-over from extracardiac sources

incomplete at the time of redistribution imaging, a resting injection can be given (ideally after sublingual nitrates) with re-injection imaging after a further 60 min of redistribution [37]. This protocol is normally sufficient for the assessment of myocardial viability.

*Late imaging.* can also be performed 24 h after injection using a longer acquisition time for the assessment of myocardial viability.

*Nitrates.* If a resting injection is given, for instance in a patient referred for viability evaluation or in a patient with a severe defect of uptake in the stress images, sublingual nitroglycerine, usually at a dose of 400–800  $\mu\text{g}$ , can be administered at least 5 min beforehand in order to reduce resting hypoperfusion and to increase the correspondence of the resting images with myocardial viability. Other nitrates such as buccal isosorbide dinitrate may also be used and these are ideally given (as with the nitroglycerine) with the patient in the supine position to avoid symptomatic hypotension.

#### *$^{99\text{m}}\text{Tc}$ -sestamibi and -tetrofosmin*

Unlike  $^{201}\text{Tl}$ , sestamibi and tetrofosmin are essentially fixed in the myocardium with no redistribution, and separate injections are given in order to assess stress and resting perfusion. The 6-h half-life of  $^{99\text{m}}\text{Tc}$  means that the two studies should ideally be performed on separate days to allow for the decay of activity from the first injection. However, as with  $^{201}\text{Tl}$ , different imaging protocols can be followed: 2-day, same-day stress–rest or same-day rest–stress:

*Two-day protocol.* A 2-day protocol is preferable because it provides good quality images obtained using the same administered activity for each. This not only facilitates

comparison between them but offers the same image quality while keeping the total radiation burden to the patient (and the staff) at a lower level compared with same-day protocols. The stress study should usually be performed first, since the rest study can be omitted if the stress study is interpreted as normal.

*One-day protocol.* The order of studies in a single-day protocol depends to some extent on the indication for the investigation. If the problem is to detect viable myocardium and reversibility of a defect, in a patient with previous infarction, it may be theoretically preferable to perform the resting study first. Conversely, when the study is performed for the diagnosis of myocardial ischaemia, the stress study should be performed first because this avoids reduction of the contrast of a stress-induced defect by a previous normal resting study [38] and also obviates the need for resting imaging.

*Imaging.* should begin 30–60 min after injection to allow for hepatobiliary clearance; longer delays are required for resting images and for stress with vasodilators alone because of the risk of higher subdiaphragmatic  $^{99\text{m}}\text{Tc}$  activity.

*Nitrates.* As with  $^{201}\text{Tl}$ , resting injections can be given under nitrate cover; this is important when assessing myocardial viability because the absence of redistribution means that viability is underestimated in areas with reduced resting perfusion [13, 14].

*Fluid intake.* can be used to remove intestinal activity from the subdiaphragmatic region. Moreover, in some centres a fatty meal is given between injection and imaging to aid clearance of tracer from the liver and gall-bladder. The value of this manoeuvre, however, is uncertain, and it may be counterproductive if there is retrograde passage of tracer from duodenum to stomach or if the tracer reaches the transverse colon [39, 40].

### Dual-isotope imaging

This protocol is sometimes used to shorten the duration of a full stress rest or stress redistribution protocol, and also to take advantage of the superior ability of  $^{201}\text{Tl}$  to assess myocardial viability at the same time as using technetium to provide functional information from ECG-gated imaging [41].  $^{201}\text{Tl}$  is injected at rest with imaging at 30–120 min, and sestamibi or tetrofosmin is then used for stress imaging. The disadvantages are the added expense and radiation burden of the two tracers, and the fact that changes between stress and rest mean that images of different tracers with different technical characteristics are compared, with lack of the possibility of performing attenuation/scatter compensation (cf. Sect. “Attenuation and scatter compensation”).

## 6. Image acquisition

### Gamma camera system

**Detectors.** Myocardial perfusion imaging may be performed using a single detector system but a dual- or triple-head system is now the state of the art to reduce acquisition time and thus the risk of patient motion. Dual-detector systems should be in a 90° or “L” configuration if they are to be used for 180° scanning.

**Crystals.** Imaging with  $^{201}\text{Tl}$  or  $^{99\text{m}}\text{Tc}$  may be performed on both thin and thicker crystals. Thick crystals up to 25 mm thick are to be used if perfusion images are performed together with FDG in order to image the 511-keV gamma rays. These detectors are generally tuned and corrected to provide good image quality down to at least the energy of  $^{99\text{m}}\text{Tc}$  (140 keV).

**Collimators.** Low-energy, all-purpose (LEAP) collimators are used for  $^{201}\text{Tl}$  studies. Low-energy, high-resolution (LEHR) collimators are most widely used and generally recommended for  $^{99\text{m}}\text{Tc}$  studies [42], but at present there is little hard evidence that LEHR, with its higher resolution, works better than the LEAP collimator, with its higher sensitivity (Table 8). LEHR collimators have a better response with depth but their reduced sensitivity tends to preclude their use with thallium [42].

**Energy windows.**  $^{201}\text{Tl}$ : 20% at 72 keV and 20% at 167 keV.  $^{99\text{m}}\text{Tc}$ : 15% at 140 keV for systems with better than 10% energy resolution and 20% at 140 keV otherwise.

### Image acquisition

#### Patient positioning

The supine position with the arms raised above the head and supported is the most commonly used position. It is important to make the patient as comfortable as possible to reduce the likelihood of motion, and it may also help to raise and support the knees.

Prone imaging may reduce patient motion and reduce attenuation of and scatter to the inferior wall [43]. If interpretation of a study obtained in the supine position is hampered by infra-diaphragmatic attenuation or scatter, an additional acquisition in the prone position may be tried. However, prone imaging may be associated with artefactual anteroseptal defects [43]. No evidence from larger series is available as to which position is better in routine work. It is important that comparison of the rest and stress studies is done with the patient in the same position, and comparison with commercially available reference populations should be done with the patient in the same, i.e. supine, position as is used in the reference population. Fe-

**Table 8.** Settings of acquisition parameters

Parameters	$^{201}\text{Tl}$	$^{99\text{m}}\text{Tc}$
Collimators	LEGP	LEHR (generally recommended, but hard evidence for its superiority over LEGP is limited)
Energy windows	20%	15% (if energy resolution exceeds 10%, use 20%)
Rotation: single or dual heads	180°	
Rotation: triple heads	360°	
No. of projections, 180° orbit	32 or 64	64–128
No. of projections, 360° orbit		128
s/projection: $^{201}\text{Tl}$ : stress/rest	20/25 s	
s/projection: $^{99\text{m}}\text{Tc}$ 2-day protocol; e.g. with dual head, 600 MBq		25 s
s/projection $^{99\text{m}}\text{Tc}$ 1-day protocol; e.g. with dual head, 350 and 1,050 MBq resp.	First scan: 25 s Second scan: 20 s	

The shown commonly recommended values refer to myocardial perfusion SPECT studies with dual- or triple-head detectors. Several of the recommendations are based on tradition and/or phantom studies whereas only a few patient studies have documented the superiority of one setting compared with other possibilities. Variations in optimal settings may also be related to different camera systems, radiotracer activities and patient characteristics

male patients should be imaged without wearing a bra. In some departments a chest band to minimise breast attenuation and to ensure reproducible positioning during later image acquisition is used for all women, while in other places it is employed only as an adjunct in special cases. The reproducible positioning is the key issue. Careful attention to technique is required when applying the band in order not to increase attenuation. It is also possible to use a chest band for males to reduce motion.

## Orbit

*180° or 360° rotation.* For single- and dual-detector systems, rotation from 45° right anterior oblique to 45° left posterior oblique is used. For a 180° acquisition, dual detectors should be in a 90° or “L” configuration. For triple-head systems, 360° rotation is used. 180° acquisitions generally give higher contrast resolution but more geometric distortions than the 360° orbit. This is especially true for the relatively low energy photons from  $^{201}\text{Tl}$ .

*Circular and non-circular (elliptical) rotation.* Non-circular orbits have the advantage of minimising the distance between the patient and the camera throughout the scan but may suffer from reconstruction artefacts due to changes in spatial resolution [44]. Data in favour of the circular orbit did not take into account the recent software compensations for variations in resolution with distance from the patient.

*Pixel and matrix size.* Pixel size is  $6.4 \pm 0.4$  mm for a  $64 \times 64$  image matrix. Zoom should be performed as necessary for cameras with a large field of view. This provides a good balance between image resolution and image noise.

## Acquisition type

Step-and-shoot is the most common mode but it may be an advantage to use “continuous step and shoot” or continuous mode if available. These continuous modes slightly improve count statistics for a given overall scan time at the cost of a slight loss of angular resolution, but the differences are minimal.

*Number of projections.* For  $^{201}\text{Tl}$  it is sufficient to use 32 views over 180°, but 64 views may be used. For  $^{99\text{m}}\text{Tc}$ , 64 or 128 views over 180° or 128 views over 360° are recommended [45].

*Time per projection.* The time per projection is always a compromise between improved count statistics and increasing the risk of patient movement. It is recommended that the overall acquisition time be kept below 20–30 min. Gating (cf. Sect. “Gated myocardial perfusion imaging”) and compensation for attenuation and scatter (cf. Sect. “Attenuation and scatter compensation”) will slightly prolong the study time.

*Attenuation/scatter compensation.* If a transmission scan for attenuation/scatter compensation is interleaved, it will prolong the time per step, typically in the range of 5 s/step. If it is not interleaved (before may be better than after, because of the greater risk of patient motion after the longer-lasting emission), the acquisition time will often be prolonged by 5–10 min.

## 7. Quality control

Quality control involves:

- The gamma camera performance in planar mode
- The gamma camera performance in SPECT mode
- Calibrations specific to SPECT
- Acquired, original data
- Processed data

### Gamma camera system

Table 9 shows the main aspects of quality control for the gamma camera and is followed by more specific details. The schedule of quality control tests and the frequency of tests should conform to national guidelines and requirements. Quality control procedures can be found in national and international guidelines [46–49]. The “IAEA Quality Control Atlas for Scintillation Camera Systems” is a useful guide for assessing quality control results and possible problems [50]. Table 10 summarises general limits that should be respected.

### Uniformity with $^{99\text{m}}\text{Tc}$ and $^{201}\text{Tl}$

- Intrinsic uniformity for  $^{99\text{m}}\text{Tc}$  should produce NEMA differential uniformity parameters within the centre field of view as close as possible to 1–2%.
- An extrinsic measurement of differential uniformity should be in the range 2–3%. For most camera systems a high count uniformity correction map (sensitivity map) is required to achieve this, and such a correction map is an essential part of the uniformity performance. The manufacturer’s recommendations for collection of this map must be followed. Care must be taken to ensure use of a proper radioactive source and use of the same energy window setting as will be used clinically.
- A statistically valid quantitative uniformity measurement, which can be reliably monitored, should be obtained from:
  - An image containing about 10,000 counts per pixel (achieved by a 30-million count image acquired in a  $64 \times 64$  matrix)
  - A 120-million count image acquired in a  $128 \times 128$  matrix.

**Table 9.** Scintillation camera quality control

Quality control of the SPECT system	Requirements
Performance of the scintillation camera	Within the manufacturer's specifications. Usually measured according to the National Electrical Manufacturers Association (NEMA) [51]
Multiple head detectors	Performance must be matched. Images from the heads aligned.
Collimators	Collimator hole angulation: at acceptance and periodically thereafter for damage
Routine quality control	Daily: symmetry of energy window position over the photopeak Daily: low count uniformity Weekly: high count uniformity and quantification Monthly: spatial resolution, linearity Periodically: total performance with SPECT phantom
Calibrations and SPECT-related quality control	High count uniformity map Centre of rotation Pixel size Detector head tilt Frequency dependent on stability of system

This quality control check should be performed weekly. On a daily basis a low count flood image (e.g. total of 3–10 million counts) is sufficient to check for any obvious changes. If  $^{201}\text{Tl}$  myocardial perfusion is performed, then the uniformity for  $^{201}\text{Tl}$  must additionally be checked. A correction map using a  $^{99\text{m}}\text{Tc}$  source may be sufficient. If not, a  $^{201}\text{Tl}$  correction map generated using a  $^{201}\text{Tl}$  source will be required.

Validity of the uniformity should be tested periodically by performing a  $360^\circ$  SPECT study of a cylinder filled with

**Table 10.** Summary of quality control for multiple head SPECT systems

Parameters	Limits to be observed
• Uniformity (NEMA)	
• Intrinsic	$\leq 2\%$
• Extrinsic	$\leq 3\%$
Maximum difference in system sensitivity between heads	$< 5\%$
Centre of rotation (COR) offset (128×128 matrix)	$< 0.5$ pixel for $360^\circ$
Alignment of heads	Perfect match
Tilt of detector heads, measured by COR (128×128 matrix)	Variation $< 4$ mm/1 pixel for $360^\circ$

a uniform solution of  $^{99\text{m}}\text{Tc}$  or  $^{201}\text{Tl}$  using the same energy window and zoom factor as are used clinically. A typical acquisition is:

- 64×64 matrix
- Same pixel size as is used clinically
- Total of 60 projections
- $360^\circ$  rotation
- 500,000 counts per projection for a phantom 20 cm long

Reconstruction with the clinically used smoothing filter should produce transverse slices that show no obvious rings (if a single detector is tested) or partial rings (if a combination of detectors is tested). This check of SPECT uniformity is useful at any time that non-uniformity is suspected.

### Sensitivity

For multiple detector systems, the sensitivity of the collimated detector heads should not differ by more than 5%.

### Centre of rotation

Centre of rotation (COR) calibration must be performed according to the manufacturer's recommendations. The results should be within the limits specified by the manufacturer. In general, the COR should:

- Not vary by more than 0.5 pixel (for a 128×128 matrix) over  $360^\circ$
- Be within 0.5 pixels of the previous measurement.

The frequency of this calibration is dependent on the stability of the SPECT system.

The validity of the COR correction can be tested periodically by measuring the full-width at half-maximum (FWHM) spatial resolution from a  $360^\circ$  SPECT study of a point or line source of  $^{99\text{m}}\text{Tc}$  or  $^{201}\text{Tl}$ . After reconstructing with a ramp filter, the SPECT resolution measured from transverse slices should be within 10% of the FWHM spatial resolution measured from a planar image of the source obtained at the same radius of rotation. In order to quantify the spatial resolution reliably, a large matrix size and a zoom factor need to be applied.

### Multiple detector head alignment

For dual- and triple-detector SPECT systems, the size and location of images produced by each head must match exactly in both the  $x$  and  $y$  directions. This means that the gain and offset of each image within the matrix must be identical. Some manufacturers include this as part of the COR calibration. A simple, but not very sensitive, test to

check the validity of head alignment is to acquire a SPECT study of a point source using the same acquisition technique as is used clinically and to review the sinogram of the raw data. There should be no jump in data in either the  $x$  or the  $y$  direction.

Another relatively simple test for head alignment is to perform a COR measurement with one head at a minimum radius of rotation and the other at the maximum radius of rotation (for locked 90° dual-head systems, this would require two acquisitions). Data from each head should be reconstructed separately. Head-1 transaxial images are subtracted from head-2 transaxial images. The results will be “doughnut” images if the heads are aligned. Note: this test can also detect errors due to collimator hole misalignment.

#### Detector head tilt

The detector head(s) must remain parallel to the axis of rotation during acquisitions. From the COR study, check that the Y-centre of mass of the point source does not vary by more than 3–4 mm over 360° (~1 pixel for a 128×128 matrix). In addition, for most single-head systems, detector head tilt can be checked using a simple spirit level. Adjust the detector head to be level at 0°. Rotate the detector 180° and again check that it is level. On multi-head systems, the COR study remains the easiest way of checking for head tilt. The summed image of all the projection views will show the point source images lying along the same row of pixels in the  $y$  direction if there is no tilt [52]. A head tilt will produce a sinusoidal pattern.

#### *The acquired, original and processed data*

The acquired myocardial perfusion data must be reviewed immediately after acquisition and before the patient leaves the department. A decision must be made as to whether the data are acceptable and any detected problem can be corrected, or whether the acquisition has to be repeated. At a minimum, the review should be made with the rotating cinematic review of the projection data and a sinogram at the level of the myocardium.

#### Ungated data acquisition

The data should be reviewed for the following:

- Complete data within the set of projection views (no blank/corrupted views)
- Expected count content of the study
- Problems related to detectors (e.g. drift in energy window, unexpected detector artefacts)
- Smooth transition of images between projections and detector heads (for multiple-head acquisition)
- Attenuation artefacts—consider whether repeated acquisition is relevant after a time interval ( $^{201}\text{Tl}$  rest study and  $^{99\text{m}}\text{Tc}$  rest or stress studies)

- Presence of extracardiac “hot spots” so close to the left ventricle that they interfere with reconstruction and processing (e.g. lung, liver, gall-bladder, muscle)—consider whether repeated acquisition is relevant after a time interval ( $^{201}\text{Tl}$  rest study and  $^{99\text{m}}\text{Tc}$  rest or stress studies)
- Patient motion—lateral or vertical movement of the myocardium on the cinematic review
- Unusual activity (e.g. injection site, arms at the side of the body)
- Truncation of cardiac activity or severe truncation of body activity
- Consistent positioning (e.g. prone or supine, feet in or feet out)

For quality control regarding gated data, cf. Sect. “[Gated myocardial perfusion imaging](#)”; for attenuation and scatter compensation, cf. Sect. “[Attenuation and scatter compensation](#)”; for reconstruction and processing, cf. Sect. “[Reconstruction methods](#)”; and for display, cf. Sect. “[Reports, image display](#)”.

## 8. Reconstruction methods

Myocardial perfusion images appear relatively uncomplicated, but they are highly processed and their appearance results from a complex interaction of the various processes. Although sophisticated reconstruction methods are available, including corrections for motion, attenuation and scatter, these software tools cannot produce “miracles”. It is therefore of importance to achieve the highest quality of the raw data before the patient leaves the department and before reconstruction is commenced (cf. Sect. “[Quality control](#)”).

Given the measured projection data, which are essentially line integrals of counts along bins for a certain angular direction, the reconstruction task is to produce an image of the activity that as closely as possible reflects the tracer distribution when the measured data were acquired. Today, two main categories of reconstruction method are available:

- The analytical or filtered back-projection (FBP) method
- The iterative reconstruction method

Properties of, and recommendations regarding, the methods are summarised in Table 11.

#### *Filtered back-projection (Table 11)*

Historically, FBP has been the main method of reconstruction used in SPECT as it was adapted from techniques used previously in other fields such as radioastronomy and electron microscopy [53]. FBP has the advantages of being fast and relatively computationally non-intensive. However, it takes no account of the basic physical processes underpinning emission tomography, which can be incorporated into the alternative statistical algorithms. Correction for

**Table 11.** Summary of properties of, and recommendations regarding, the more common filtering techniques applied in myocardial perfusion SPECT

Operation and properties	Recommendations
FBP: fast, computationally non-intensive. Cannot incorporate attenuation and scatter correction in the reconstruction	Recommended filter cut-off values should be expressed as proportion of the Nyquist frequency. Nyquist frequency is $0.5d$ , where $d$ is the pixel size in cm, i.e. half the sampling frequency. For example, if the pixel size is 6 mm, the Nyquist frequency is $0.8 \text{ cm}^{-1}$ For comparison between different vendors, check that filter parameters are defined equally Best left with cut-off at 1.0
Ramp filter: weights the data for reconstruction proportional to their spatial frequencies	
Low-pass filters: roll-off at high spatial frequencies to reduce ringing artefacts and constrain amplification of noise	Optimisation of filter parameters is best carried out empirically by each department based on their normal acquisition parameters Filter cut-offs should not be varied routinely
Butterworth: care should be taken that the manufacturer has correctly defined the cut-off point. This should be where the amplitude drops to $1/\sqrt{2}$	<i>Radioisotope (power: <math>n=6</math>); fraction; Nyquist<sup>a,b</sup>:</i> <sup>201</sup> Tl; 75 MBq; 0.3–0.4 <sup>99m</sup> Tc; 500 MBq; 0.3–0.4 <sup>99m</sup> Tc; 1,000 MBq; 0.4–0.5 <sup>99m</sup> Tc; 1,500 MBq; 0.5–0.7
Hamming: this is the generalised Hamming window function with $\alpha=0.5$	<i>Radioisotope (power: <math>=6</math>); fraction; Nyquist<sup>a,b</sup>:</i> <sup>201</sup> Tl; 75 MBq; 0.25–0.40 <sup>99m</sup> Tc; 500 MBq; 0.30–0.45 <sup>99m</sup> Tc; 1,000 MBq; 0.45–0.60 <sup>99m</sup> Tc; 1,500 MBq; 0.60–0.80
Wiener and Metz: resolution recovery filters which constrain the inverse filter at high spatial frequencies	Should only be used by persons with a thorough understanding of the underlying theory
Others: these can include functions such as the Parzen and Shepp-Logan	Best avoided as the Butterworth and Hamming filters are now widely available
Iterative reconstruction: allow incorporation of physical effects such as attenuation, scatter and collimator response, but fixed point of convergence	Noisy data need to be low-pass filtered prior to (2D) or after reconstruction (3D). For quantitative studies, programs must be linear, i.e. total counts equal before and after reconstruction
Maximum likelihood expectation maximisation (MLEM): most software recommends 10–15 iterations	Too many iterations tends to amplify noise. Too few reduce image quality and resolution
Ordered subsets expectation maximisation (OSEM): acceleration roughly a factor equal to the angles/subsets. One to two may be sufficient	For practical application useful but do not theoretically always converge

<sup>a</sup>The figures given are based on a pixel size of 6 mm

these effects needs to be made pre- or post-reconstruction. Hence, although FBP is probably still (2004) the most frequently used method of SPECT reconstruction, it is rapidly losing ground to the iterative techniques.

The filters most commonly used in FBP are generally low-pass filters such as the Hanning and Butterworth combined with the required ramp filter. These low-pass filters reduce the high spatial frequency components of the image and thus reduce the noise though at the expense of the spatial resolution in the image. In general, the cut-off frequency and power factors (if necessary) may follow the recommendations of the vendors if standard activity amounts of radionuclide tracers and imaging techniques are applied, although ideally they should be determined empirically by each department. Such evaluation should be based on the count statistics of an average study produced by the department's normal acquisition protocol. The chosen filter should produce images of similar quality over a reasonable

range of count levels around the average value. Optimisation should be based on data presented and assessed in the prevailing format used for reporting of the studies.

Two issues are particularly important in FBP:

- How are negative numbers handled that occur in the reconstructed images because of ramp filtering?
- The most common method is to truncate these values to zero. However, this results in loss of the linearity in the reconstruction process (e.g. same number of counts in the reconstructed images as have been acquired), which is important in procedures where an absolute activity quantification is important (volume determination in gated studies).
- FBP does not eliminate streak artefacts completely, which means that counts will appear outside the body region in the SPECT image, as seen in Fig. 4. Streak artefacts should be recognised in the image as such and

ignored; software manipulation to try to remove them is not recommended.

#### Iterative reconstruction methods (Table 11)

This family of reconstruction methods [54] has been clinically available only for the last few years. In addition to the back-projection step in FBP, there is also a forward projecting step in iterative methods. This step is required to calculate projection data (or line integrals) along a path from an image matrix defined in the computer and thus simulate the distribution for which the actual measured SPECT data were obtained. An iterative procedure starts with an initial first guess of the activity distribution (Fig. 5).

This starting point can be a flat image or an image obtained by FBP. The key feature is then the comparison between the measured projection data and the projection data calculated from the image matrix. A correction matrix is formed that is multiplied by the initial guess after proper normalisation. An updated image is created and the process has made its first iteration. The new updated version of the activity distribution can then be used as input for the same procedure to form the second and more accurate update. This is achieved since the difference between the measured and calculated projection data will decrease. After a certain number of iterations, the difference between the calculated and measured projection data is only assumed to be a function of image noise and therefore the process is stopped and the last updated image used as the final reconstructed image. The flow chart in Fig. 5 summarises these steps.

The most commonly used iterative methods in commercially available systems are the:

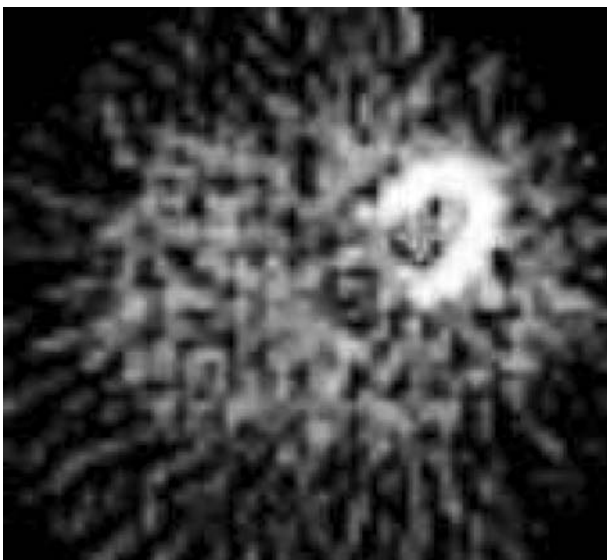


**Fig. 4.** Streak artefacts with FBP. Illustration of streak artefacts inherent to the FBP process

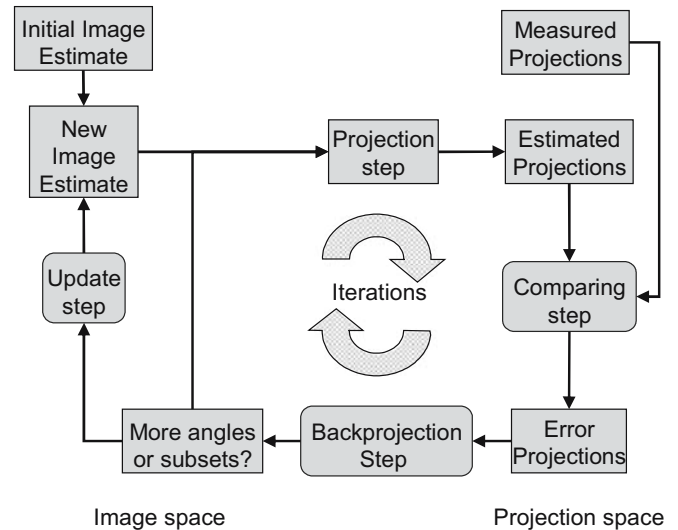


**Fig. 5.** The iterative procedure. The flow chart describes the steps of the iterative procedure

- *Maximum likelihood expectation maximisation method (commonly denoted MLEM)*, which, however, is time consuming: the image is updated (i.e. multiplied by the correction matrix) only after all projection angles have been processed.
- *Ordered subsets expectation maximisation (OSEM)*, an accelerated version [55]. The image is updated after a subset of projections has been processed. The acceleration is roughly proportional to the number of subsets.

The equation that describes the process is given by:

$$I_i^{\text{new}} = \frac{I_i^{\text{old}}}{\sum_j h_{ji}} \sum_j h_{ji} \frac{P_j}{\sum_k h_{jk} I_k^{\text{old}}}, \quad (1)$$

where  $I$  is the image to be created,  $P$  is the measured projection and  $h_{ij}$  is the probability (or the transfer matrix) that the pixel  $I$  will contribute to the projection bin  $j$ . In its simplest form, which assumes no photon attenuation, no scatter contribution or collimator blur,  $h_{ij}$  is unity along the ray-of-view for the current projection angle. This then reduces the formula to:

$$I_i^{\text{new}} = \frac{I_i^{\text{old}}}{\sum_j h_{ji}} \sum_j \frac{P_j}{\sum_k I_k^{\text{old}}}. \quad (2)$$

The summation term under Eq. 1 is needed because the back-projection step is a summation step and therefore a normalisation with the number of projection angles is essential to keep the number of counts in the reconstructed images the same as originally acquired.

An iteration is defined when all subsets are processed. The process is then repeated for the desired number of iterations. Figure 6 shows an example using images obtained with different iteration numbers for MLEM and OSEM.

In contrast to FBP, iterative methods generally do not have a clear definition of the point at which the images can be regarded as final. The number of necessary iterations

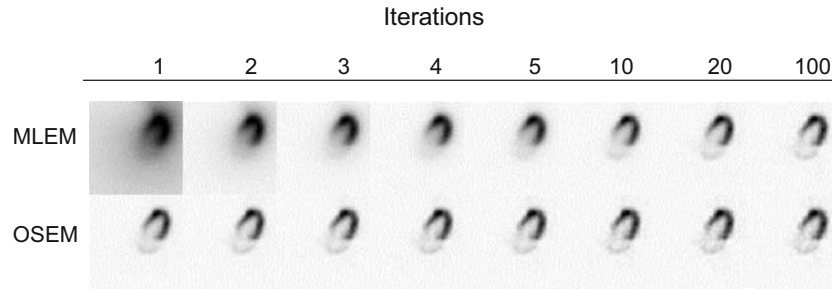


**Fig. 6.** Different iteration numbers for the MLEM and OSEM methods. Example of images obtained with different iteration numbers for MLEM in the *upper row* and OSEM in the *lower row*

depends on the method of choice and the image noise. For most cases, the rule of thumb of about 15 iterations for an MLEM procedure [56] and two iterations for OSEM can be applied, and these numbers are often recommended by commercial vendors. Low-pass Fourier filtering can introduce ring artefacts (the Gibbs phenomenon) if the filter is not properly selected. However, the iterative process is well suited to inclusion of physical effects such as photon attenuation and contributions from photons scattered in the patient. The effect of photon attenuation can be included in the  $h$  function by calculation of the exponential between the current pixel location and the surface before summation of pixel values along the ray of view. This can be done either by using a fixed attenuation coefficient or by including a matched attenuation map, obtained, for example, by transmission SPECT or from a co-registered CT study. Non-homogeneous attenuation compensation can then be incorporated in the forward projection step. The accuracy of such attenuation compensation is mostly dependent on the accuracy of the obtained attenuation values. The collimator response can be included in  $h_{ij}$  by calculating the contribution (the probability of detection) in other projection bins from voxel  $i$ .

## Conclusions

Both FBP and iterative methods are useful, but the latter are now preferred since they offer more accurate modelling of physical processes and reduce noise. In particular, it should be noted that:

- Compensations for scatter, attenuation and detector blur are difficult with FBP.
- Iterative methods allow the physical processes to be modelled in the projector step (with superior correction for non-homogeneous attenuation and detector response).
- Scatter compensation can be included either in a pre-subtraction step or preferably (due to the decreased noise problems) directly in the projector step.
- The reconstructed noise in iterative methods is less disturbing than with FBP.
- A rule of thumb is 10–15 iterations for MLEM procedures and two iterations for OSEM.

- There is no clear definition of the point at which the images can be regarded as final.

## Filtering (Table 11)

The filter cut-off should not be varied routinely. In general, low count studies (e.g.  $^{201}\text{Tl}$  compared with  $^{99\text{m}}\text{Tc}$  tracers) require smoother filters than higher count studies. However, if a study appears to suffer from unexpected low count rates, the acquisition time should instead be adjusted. Care must be exercised when filter parameters from one manufacturer's system are compared with those from another system. The mathematical definition of the filter window may vary between systems (e.g. the definition of cut-off value of the Butterworth filter). The correct definition of the cut-off for this filter is the point at which the amplitude drops to  $1/\sqrt{2}$ , or 0.707 [57]. However some manufacturers use simplified definitions of this filter, where the cut-off is the point at which the amplitude drops to 0.5, or rolls off to zero.

*Other filters.* The use of adaptive, or resolution recovery, filters should also be treated with care. These filters are used as constraining operators on the inverse filter. The inverse filter is essentially the reciprocal of the point spread response function of the camera system.

Deconvolution with this filter would in theory produce ideal images, with the degrading effects of the imaging process removed. But this would produce high levels of noise with clinical data. The adaptive filters constrain the inverse filter at high spatial frequencies and allow its use as a clinical filter.

The Metz and, more commonly, Wiener filters are the functions generally used for constraining the inverse filter. These have been shown to improve quantification with myocardial perfusion SPECT in certain cases [58]. However, the power factors for these filters are dependent upon the properties of the noise power spectrum of the data. Therefore, the choice of a single power factor that will be applicable over a clinically realistic range of count levels is problematic. The use of an incorrect power factor can lead to erroneous enhancement of sections of the image spectrum [59] and introduce apparent defects (Fig. 7). For these

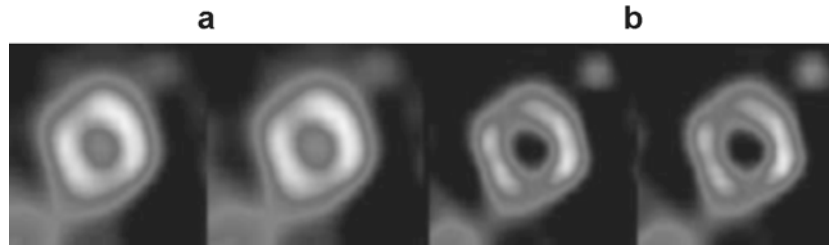


**Fig. 7.** A conventional low-pass filter (a) and a resolution-recovery filter (b). The images show the same short axis slices through a ventricle reconstructed with a conventional low-pass filter (a); apparent, but false, segmental defects are introduced with a resolution-recovery filter (b)

reasons it is probably best if these filters are avoided for data reconstruction unless a person with special expertise and clinical experience is responsible for their use.

Iterative reconstruction methods do not require a filtering step like the ramp filter in FBP. If the acquired data are noisy, one can apply a low-pass 2D filter on the projection data or a 3D post-filter on the tomographic images. The same principles as cited above are also applicable to iterative reconstruction methods.

#### *Motion correction*

A number of proprietary motion correction packages are available from manufacturers on modern gamma camera systems (Table 12). These use a variety of methods to correct for translational motion of the heart during the acquisition. Some methods use external point sources [60], whilst others use fitting to an idealised sinogram [61]. If an automated method of correction is to be used, the algorithm in use should be understood to ensure it works correctly. For example, when using some sinogram fitting techniques, the heart must be placed away from the centre of the field. If the heart does lie at the centre, then the sinogram will describe a straight line instead of a sine wave, and the algorithm may fail.

It should be noted that these methods only correct for relatively simple forms of motion such as motion in the longitudinal axis, which is usually possible with the commercial software systems. More complex patterns of motion involving rotational motion cannot be adequately corrected using current methods. This may include the relatively common phenomenon of ‘upward creep’ [62]. Previous work has demonstrated that movement by 1 pixel does not produce significant artefacts [61] in the recon-

structed images. Therefore, it is recommended that only motion by 2 pixels or greater justifies correction.

#### *Reorientation of image data*

Reorientation of the reconstructed transaxial data into the three standard image planes should always be consistent. Errors in reorientation can introduce artefacts, which may be mistaken for perfusion defects [63]. Automated methods of reorientation are available [64, 65] and have been shown to be at least as accurate as trained operators and probably to achieve greater reproducibility. Automated methods may fail in selected cases such as large myocardial infarctions and cardiac orientation abnormalities. If manual reorientation is chosen, the operators should use reproducible landmarks for definition of the long axes. Common landmarks include the apex and points on the valve plane.

## 9. Gated myocardial perfusion imaging

Two advantages may be accrued when perfusion SPECT studies are acquired in an ECG-triggered, “gated” mode:

1. Evaluation of LV ejection fraction (EF) and volumes, and evaluation of LV regional wall motion.
2. Improvement of the diagnostic accuracy of perfusion imaging [66] in the event of attenuation problems (apparently irreversible perfusion defects due to attenuation artefacts may be wrongly interpreted as scar tissue, though function is maintained).

*<sup>99m</sup>Tc tracers.* Perfusion data reflect the condition at the time of tracer injection (at rest or during stress), whereas the functional gated SPECT data represent images of the LV

**Table 12.** Motion correction and data reorientation

Properties	Recommendations
Motion correction: a number of packages are now available which use a variety of techniques	Only vertical motion is corrected by commercial programs Only patient movement $\geq 2$ pixels in the projections should be corrected
Reorientation into the three standard image planes should always be consistent	Verified automated techniques are at least as good as trained operators If manual methods are chosen, consistent landmarks should be used

myocardium during the acquisition, i.e. generally under rest conditions.

It should be noted that, although functional gated SPECT acquired after stress shows the left ventricle at rest, it may sometimes represent a different physiological state. If a patient is injected at the time of stress-induced ischaemia, transient wall motion abnormality and possibly dilated left ventricle and reduced EF (myocardial stunning) may persist and be observed during the acquisition phase, up to 90 min or even later after the resolution of ischaemia. Detection of post-stress myocardial stunning by means of gated SPECT may contain independent, important information about the left ventricle, useful for both diagnostic and prognostic assessments.

<sup>201</sup>Tl. Gated <sup>201</sup>Tl studies can be performed, but the accuracy and reliability are lower than for the <sup>99m</sup>Tc-labelled tracers.

### ECG triggering

The demands are that:

- The patient has a fairly regular heart rhythm: atrial fibrillation, sinus arrhythmia, frequent premature beats, intermittent and dual-chamber pacing etc. should not be studied with ECG triggering.
- There is adequate count density; particular care must be paid to lower activity acquisitions.

The ECG lead should be carefully chosen so that the R wave is a marker of end-diastole. The R wave must be positive in most triggering systems. Ideally, the R wave should be at least threefold higher than the P as well as the T wave and should have the steepest rising slope of the ECG cycle.

There is no clear consensus on the tolerance window for the frame/bin length in gated SPECT acquisitions: the narrower the window, the more physiological the data, but the study may suffer from low count statistics and/or from an inappropriate increase in the acquisition length. Classically, it is recommended that cardiac cycles exceeding 30–40% deviation from the averaged cycle length should be excluded for the functional information but not for the evaluation of the LV perfusion if the camera rotation is set to a fixed time duration per step (see below).

### Intervals

The cardiac cycle is usually divided into eight, and sometimes into 16 intervals (frames, bins). The lower frame rate results in a slight underestimation, by about 4 EF units, of the LVEF value [67]. Nevertheless, eight intervals seem to be a reasonable compromise between the count statistics that should provide accurate definitions of cardiac walls and the temporal resolution that is required to record the short end-systolic period. Sixteen intervals provide better determinations of LVEF and end-systolic volume (enhanced

temporal resolution), but eight intervals might provide a better assessment of regional wall motion (enhanced signal-to-noise ratio of gated SPECT images) and are probably the most frequently used value.

### Time per projection

Each step of the camera rotation may be set to a fixed time duration or a fixed number of accepted cardiac cycles. There is no hard evidence for superiority of either preset, but most groups use fixed time. In some systems, when the preset time per step is used, only the data related to the functional part are accepted/not accepted, whereas all the data are stored for perfusion processing.

Time per projection must be adjusted to obtain an adequate myocardial count rate per interval, but the total acquisition time should not exceed 30 min due to risk of patient movement. For a <sup>99m</sup>Tc-based gated study the length of acquisition should not exceed that traditionally used for a non-gated SPECT study. For a <sup>201</sup>Tl gated study, it may be necessary to extend the acquisition time, especially for gated redistribution analysis.

In Table 13 recommended examples for gated SPECT acquisitions are shown.

For gated SPECT with <sup>201</sup>Tl, count density is consistently much lower than that obtained with <sup>99m</sup>Tc-labelled tracers. A number of studies have compared gated <sup>201</sup>Tl and <sup>99m</sup>Tc studies, with acceptable LVEF values obtained with <sup>201</sup>Tl, when <sup>99m</sup>Tc is used as the gold standard [68]. However, there is no doubt that assessment of regional wall motion is more accurate with the studies obtained with <sup>99m</sup>Tc-labelled tracers [69]. To date (December 2004), no studies have demonstrated improved specificity of <sup>201</sup>Tl imaging by gating the SPECT perfusion data.

*Motion artefacts.* Gated studies are sensitive to patient motion during the acquisition, even when limited, since the exact shape of myocardial walls will be affected and lead to incorrect definitions of the endo- and epicardial borders, and wrong calculations of volumes and EF.

*Multidetector gamma cameras.* Practical considerations related to patient tolerance and avoidance of motion limits the application of gated acquisitions to multidetector cameras. The risk of low-quality gated studies on a single-headed camera is too high to justify gating.

### Image processing

#### Filtering

The choice of filters is essentially the same as that for non-gated SPECT imaging. As might be expected, a gated SPECT study needs to be smoothed a little more than a non-gated study, because of the lower counts in each of its multiple frames. But too much filtering will affect the shape and sharpness of the myocardial wall contour, resulting in

**Table 13.** Recommended duration of gated SPECT acquisition

Tracer	Activity (MBq)	No. proj./180°	s/projection	Two detectors, 90° (min)	Three detectors, 120° (min)
<sup>99m</sup> Tc tracer (low count)	300–450	60	35	18	23
<sup>99m</sup> Tc tracer (high count)	900–1,100	60	25	13	17
Stress <sup>201</sup> Tl	75–170	60	35	18	23
Redistribution <sup>201</sup> Tl	Gated imaging not recommended				

Different injected activities of <sup>201</sup>Tl- and <sup>99m</sup>Tc-labelled radiopharmaceuticals for different camera configurations, using a low-energy high-resolution collimator, 3° angular sampling, 180° acquisition and eight-frame gating [67]

an underestimation of LV size (although yielding nicer images with a high signal-to-noise ratio). Since most of the automatic programs quantifying gated SPECT perfusion data are based on edge detection algorithms and are relatively insensitive to count statistics, it is recommended always to use the same filter parameters independent of the actual count density in a given patient.

### Reconstruction

As for non-gated studies, two methods may be used: FBP and iterative reconstruction. The iterative methods are rapidly gaining wider acceptance (cf. Sects. “[Reconstruction methods](#)” and “[Attenuation and scatter compensation](#)”).

### Quality control

In addition to all the quality assurance procedures for routine SPECT, the adequacy of the ECG gating and the number of counts acquired in each interval should be evaluated, as listed in Table 14.

### Image analysis

Analysis of gated SPECT images includes the determination of LV volumes and EF, with the use of automatic edge detection software, and the visual assessment of regional wall motion and wall thickening. To date (De-

cember 2004), no program has been shown to quantify wall motion parameters in a more precise way than conventional visual analysis.

### Regional wall motion and wall thickening

The analysis should take into account physiological and pathophysiological variations such as:

- Reduced wall motion at the base compared with the apex, observed in healthy subjects
- Greater excursion of the basal lateral wall than the basal septum, observed in healthy subjects
- Paradoxical septal motion observed in patients with left bundle branch block or a ventricular pacemaker

Wall motion can be classified as normal, decreased, absent or paradoxical. Computer-generated contours can be helpful, but these should not be used as the sole determinant of motion.

Wall thickening is assessed according to the relative increase in myocardial counts between diastole and systole (partial volume effect). Computer-generated contours can be helpful, but these should not be used as the sole determinant of thickening. Thickening can be classified as normal, reduced or absent.

It is commonly accepted that wall motion and wall thickening may be incorporated into a single qualification while noting the discordance between motion and thickening when it occurs. For instance, such discordance is commonly observed in the septal wall after coronary bypass surgery and in right ventricular overload: wall motion is decreased, whereas wall thickening is preserved.

- A *normal* regional function is defined when wall thickening and motion are normal.
- A *hypokinetic* region is defined when wall thickening and/or motion is decreased.
- An *akinetic* region is defined by absence of wall thickening and motion.
- A *dyskinetic* region is defined by absence of wall thickening and paradoxical wall motion (Fig. 8).

**Table 14.** Quality control of gated studies

Parameter	Items that should be checked
Heart rate histogram	Only one “narrow” peak
Analysis of LV volume curve	End-systole $\leq 2$ frames within first half of cardiac cycle End of curve (almost) on level of onset of curve
Cine inspection of contracting left ventricle	Correct positioning of diastole in cardiac cycle No frames with reduced counts
If automatic edge detection	Correct endocardial and epicardial edge definitions

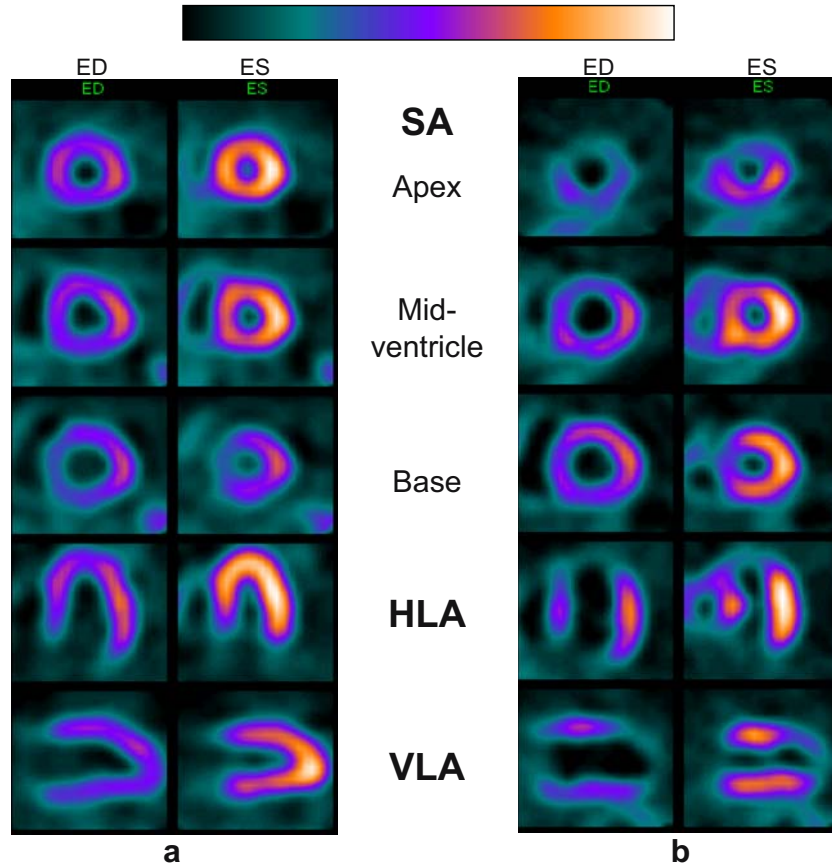


**Fig. 8.** Examples of normal (a) and abnormal (b) regional function. Slices of two left ventricles in end-diastole (ED) and end-systole (ES) on three levels (from apex to base) in the short axis (SA), one level in the horizontal long axis (HLA) and one level in the vertical

long axis (VLA). **a** Normal regional wall motion and thickening. **b** In a patient with recent myocardial infarction, wall motion and thickening are severely impaired in the anterior wall and apex

#### Left ventricular EF and volumes

LV end-diastolic volume, end-systolic volume, stroke volume and EF are calculated automatically with the use of well-validated contour detection programs. Caution should be exercised in reporting apparently spurious values of these parameters. For instance, volumes are often too low and EF too high in small ventricles. Reporting of volumes may preferably be indexed according to body surface area, since the reference values have a narrower range. Normal limits of LVEF and volumes measured with gated SPECT are influenced by the number of frames, the tracer and the algorithm used. Reference limits obtained with the QGS software, eight frames and a  $^{99m}\text{Tc}$  perfusion tracer are listed in Table 15.

#### Image display

See also Sect. “Reports, image display”.

As a minimum, the display of gated SPECT should include apical, mid-ventricular and basal short axis, and mid-ventricular horizontal and vertical long axis slices in end-diastole and end-systole. Regional wall motion and wall thickening may be analysed with the use of a single

colour linear scale, such as a grey scale. A linear grey scale without computer-derived edges has been suggested to be the best display for evaluation [67]. A continuous colour scale may be better for evaluation of regional wall thickening.

#### Integration of LV perfusion and functional data

The results of non-gated perfusion and gated LV function from the SPECT examination should be integrated to reach a final interpretation:

- Integrate analyses of perfusion and functional data for the same, well-identified LV regions.

**Table 15.** Reference lower limits of post-stress LVEF and volumes (QGS; eight frames;  $^{99m}\text{Tc}$  tracer) [70]

Gender	LVEF (%)	EDVI ( $\text{ml}/\text{m}^2$ )	ESVI ( $\text{ml}/\text{m}^2$ )
Female/male	50/45	56/70	25/32

EDVI end-diastolic volume index, ESVI end-systolic volume index, LVEF left ventricular ejection fraction

- LV functional data should not be interpreted in too small segments owing to the risk of passive motion/impression of thickening in neighbouring segments, etc.
- Wall motion/wall thickening present in apparently fixed perfusion defects may help in the discrimination of infarction from attenuation artefact. The number of equivocal interpretations [71] is reduced.
- Post-stress regional LV dysfunction not present in rest images (myocardial stunning) improves sensitivity for detection of severe coronary artery disease [72]. Post-stress LV dysfunction has independent prognostic value [73].

## 10. Attenuation and scatter compensation

In addition to pixel size, type of orbit etc., primary factors of concern for image quality are:

- *Attenuation* of radiation in the body, which can lead to a non-uniform reduction in the apparent activity in the myocardium and to the introduction of artefacts in the images.
- *Scatter* of radiation both within the body and in the detector, which degrades image contrast and potentially affects quantitation of activity and relative distribution of perfusion.
- Changes in *resolution* with distance from the collimator face, which can alter the apparent distribution of activity in the myocardium.

The issue is quite complex:

- Attenuation is considered to have the most significant effect [63, 74–84].
- Early clinical studies were disappointing: Failure to incorporate effects of scatter into the attenuation compensation (AC) technique may result in over-compensation of the data and introduction of artefacts.
- Most commercial camera systems now offer a combination of both software and hardware for non-uniform AC.
- Software and hardware methods used in these systems vary significantly from one vendor to another.

It is documented that compensation with at least some systems does improve image quality and image interpretation. Because of the rather fast development within the technology and the significantly different requirements of the current commercially available AC techniques, it is not possible at present to set exact guidelines as to how AC studies should be performed [85].

Hence these guidelines attempt to define the key aspects of AC techniques that should be considered when using these techniques in clinical practice. Many of the existing systems still do not include the option of well-functioning AC.

### *Attenuation compensation*

The amount of attenuation in a clinical study depends on several factors, including:

- The type of tissue (soft tissue, bone or lung)
- The energy of the radiation
- The thickness of the body

Hence, compensation for soft tissue attenuation requires exact knowledge of the attenuation characteristics for each patient. While many schemes for the generation of the attenuation characteristics have been reported, nowadays the attenuation map of a patient is usually generated by transmission imaging, using an external radiation source. Commercial systems have employed:

- Gadolinium-153 (100 keV)
- Americium-241 (60 keV)
- Barium-133 (356, 81 keV; 302, 383 and 276 keV)
- Cobalt-57 (122 and 136 keV)
- Technetium-99m (140 keV)
- CT-type devices

Because of the variety of techniques used to generate attenuation maps of the body, it is important to be aware of the technical factors that influence the quality of the attenuation map. Specific guidelines for each vendor's system should be consulted with respect to a number of factors (Table 16).

### *Scatter compensation*

Most AC maps are generated by techniques that minimise scatter in the transmission data. Therefore these maps provide attenuation coefficients applicable to scatter-free emission data. Unfortunately, emission data usually contain a significant percentage of scattered events. Hence in order to be able to apply the attenuation map to the emission data, some adjustment or correction must be made to either the emission data or the attenuation map. A wide range of algorithms is in use for scatter compensation, and there are few data to support the use of any one specific algorithm [86]. Specific guidelines for each vendor's system should be consulted.

Scatter compensation on the emission data can be performed by:

- Use of one or more additional energy windows (to model the scatter component)
- A reduction in the primary energy window to minimise scatter
- Modelling of the scatter based on the emission data
- Empirical determination of an effective attenuation coefficient

The use of additional energy windows or a reduction in the width of the energy window will increase noise in the

**Table 16.** Parameters of importance for the performance of an AC system

Parameters	Check list
Transmission source strength	Minimum source strength or count rate? Sources with a limited half-life (e.g. $^{153}\text{Gd}$ ): when should the source be replaced? When is it inadequate for AC?
Truncation of attenuation map in obese patients	Partial truncation of the patient in transmission beam, if the girth of the patient is greater than the field of view: how does the system handle that?
High count rates in small patients	How does the system handle potentially high count rates associated with minimal attenuation (high count rates may lead to count loss, resulting in an overestimation of the attenuation coefficients)
Simultaneous or sequential transmission	Simultaneous: is there correction for cross-talk between the emission and transmission energy windows, and how has this been validated? Sequential: is there ability to correct for patient motion between emission and transmission scans?
Quality control (QC) of transmission system	Moving line or point transmission sources: is there a quality control procedure available to check the accuracy of movement of the sources?
QC of X-ray source	Is there a QC procedure to ensure that the X-ray system is operating correctly? Is there ability to check the accuracy of co-registration of X-ray and emission data?
Accuracy of down-scatter correction for $^{153}\text{Gd}$	Important for 1-day protocols where magnitude of correction may differ by a factor of 3–4 between low-dose and high-dose studies [91]

image data. Noise-related non-uniformities may negate any advantage of AC. Modelling of the scatter is potentially the most attractive option as it does not incorporate additional noise into the data [86].

#### *Loss of resolution with depth*

A number of other factors may influence the quality of myocardial perfusion studies. Acquisition parameters such as type of collimation, type of orbit and acquisition arc all affect spatial resolution and result in changes in the resolution of the images with rotation. Depth-dependent resolution recovery algorithms are employed on some commercial systems [87]. The purpose of depth-dependent resolution recovery algorithms is to improve the uniformity of resolution over the myocardium. The accuracy and validity of these algorithms has not been well studied. However, compensating for changes in resolution should further improve the overall detection of coronary disease [88].

#### Process of attenuation compensation

It is also important to consider at what point the various compensations described above are applied to the data. An iterative algorithm that incorporates compensations for attenuation, scatter and loss of resolution with depth may perform better than programs that consider these compensations separately. For example, a scatter subtraction program may generate more noise than an MLEM algorithm that includes a measured or modelled scatter estimate. Likewise, streak artefacts and negative pixel values with FBP may be poorly handled by a separate AC program.

#### Validation of attenuation compensation devices

Any site contemplating the clinical use of AC in cardiac studies should perform some basic performance testing of the AC device, which should comprise at least two phantom imaging experiments [89]: a suitable myocardial phantom and an anthropomorphic phantom.

1. The myocardial phantom should be filled with the appropriate radioisotope ( $^{99m}\text{Tc}$  or  $^{201}\text{Tl}$ ). The LV cavity should be empty. The myocardium should be suspended in air and orientated as if in a patient. The gamma camera should perform a standard cardiac SPECT acquisition as would be performed in an AC study. No AC should be performed.
2. The left ventricle should then be filled with water and the myocardial phantom placed inside an anthropomorphic phantom. An AC study should be performed and the impact of AC, both with and without additional corrections for scatter and resolution recovery, should be assessed. Although there will be some minor self-attenuation within the walls of the myocardium, the uniformity of the myocardial phantom in air should serve as a good benchmark against which to compare the AC algorithm.

Because of the large variations in body size and composition, phantom studies cannot show all the potential problems with an AC device. Hence, non-AC and AC data should be viewed side by side to enable the reviewer to determine changes in image quality resulting from the AC device (Fig. 9). In addition, the reviewer should evaluate the planar transmission data for soft tissue truncation or high count shine-through, and check the quality of the attenuation map for errors in downscatter correction or for

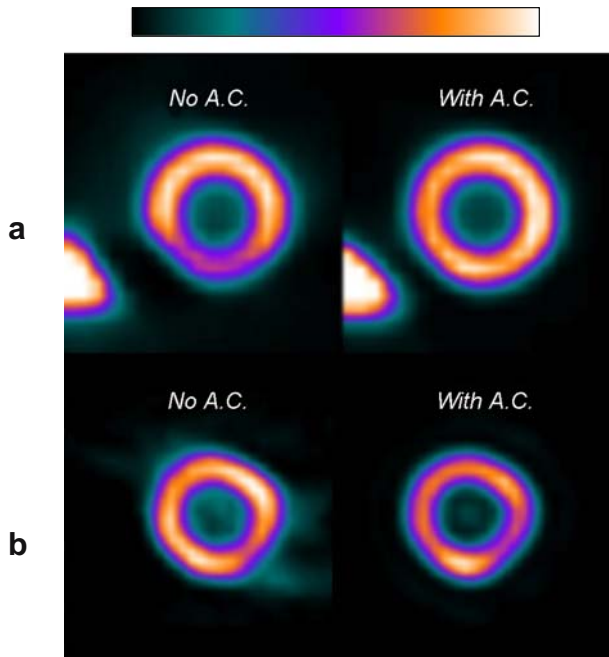


**Fig. 9.** Attenuation and scatter compensation of short axis slices from a normal myocardium in a cardiac phantom. **a** The presence of an adjacent hot liver ( $\times 2$  myocardial activity) results in artefacts in the FBP images, which are corrected after application of AC. **b** Increased non-uniformity is shown in the attenuation-compensated images relative to those seen in the FBP images, owing to an error in the AC algorithm

changes in the measured attenuation coefficients due to a weak transmission source. A simple check of the attenuation map can be done using region of interest analysis to determine the average attenuation coefficients for soft tissue, lung and bone. It is necessary to consult the manufacturer's documentation to determine how to convert a pixel value to an attenuation coefficient (usually a simple multiplier).

#### Application in clinical practice

Several large multicentre trials have demonstrated that the primary advantages of AC are increased specificity and normalcy rates [85]. While AC is of most value in resolving the true nature of fixed defects, variations in hepatic and bowel activity as well as variability in the position of the breast in women may also make it of value in patients with reversible defects [90]. A major factor to be considered when incorporating AC data into clinical practice is that many trained physicians mentally perform an internal AC. Hence they may need to review both the non-AC and the AC images in order to relearn the appearance of a normal myocardium, as well as understand any residual artefacts or limitations not compensated by the vendor's AC program.

#### Summary of recommendations

- Attenuation and scatter compensation has been shown to improve the quality of images and the interpretation of patient studies.
- The function of attenuation and scatter compensation is highly dependent on the specific hardware and algorithms applied.
- Attenuation compensation without scatter compensation cannot be recommended.
- Validation of attenuation and scatter compensation must include phantom studies before clinical use.
- Patient studies should always comprise both compensated and non-compensated data sets, viewed side by side.
- The laboratory must establish their own QC program for the acquisition, analysis and review of AC studies, based initially on the recommendations from the equipment vendor.

## 11. Data analysis

For adequate interpretation of myocardial perfusion images, a systematic visual review of raw data and reconstructed images on a computer screen is warranted. The system of reviewing comprises several reviewing levels of increasing complexity:

- Simple analysis of raw data (quality control)
- Stress parameters
- Processed image data (without and, if available, with attenuation/scatter compensation and gated cine data)
- Quantitative data (incl. comparison with reference databases)
- Integration with clinical data

Apart from the additional information generated, quantitative analysis and information from gated images are valuable supplements to the visual interpretation of perfusion data.

#### Visual interpretation

##### Review of original ("raw") data

- Inspection and review of stress and rest raw data alongside each other, also in cine mode, are important for quality control (Table 17).
- Results of gated studies.

In addition to the quality control, inspection of raw data may give additional useful information about:

- Evidence of LV dilatation, either permanent or transient after stress.

**Table 17.** Quality control

Quality control of artefacts	Comments on possible artefacts in raw images
Patient motion	Use motion correction (cf. Sect. “ <a href="#">Reconstruction methods</a> ”)
Upward creep	In particular with $^{201}\text{Tl}$ , review cine. Use motion correction (cf. Sect. “ <a href="#">Reconstruction methods</a> ”)
Soft tissue attenuation	Inferior wall in males Breast attenuation in females and pectoral muscles in athletic subjects Attenuation/scatter compensation (cf. Sect. “ <a href="#">Attenuation and scatter compensation</a> ”)
Scatter	Adjacent activity in: Bowel Liver Gall-bladder (cf. Sect. “ <a href="#">Attenuation and scatter compensation</a> ”)
Irregular heart rhythm	Gated images should not be used if low count density occurs in some projection images (most often due to significant rejection of cardiac cycles, cf. Sect. “ <a href="#">Gated myocardial perfusion imaging</a> ”)

- Increased lung uptake of tracer, particularly  $^{201}\text{Tl}$ .
- Right ventricular uptake, which suggests right ventricular hypertrophy or, occasionally, generalised reduction of LV uptake.
- Extra-cardiac abnormalities: focal breast or lung accumulations, duodenal-gastric reflux and bile obstruction.
- Integration with rest and stress haemodynamic data. Lack of true rest in patients with critical coronary disease may also lead to underestimation of the presence, severity and extent of reversible perfusion defects. Inadequate stress may underestimate the presence, severity and extent of stress-induced perfusion abnormalities.

#### Review of tomograms

*Slices.* All three image planes should be inspected: short axis, horizontal long axis and vertical long axis. Stress and rest images should be aligned in a way that the tomograms are carefully displayed with anatomically corresponding stress and rest slices under each other, from apex to base. Preferably, a format that allows simultaneous inspection of the three image planes is used. A continuous colour scale should be used. If attenuation/scatter compensation has been applied, both images with and images without compensation should be evaluated (cf. Sect. “[Reports, image display](#)”).

*Polar maps (bull's eye) display.* LV perfusion in a single two-dimensional image. This display facilitates assessment

of the presence, extent and location of perfusion abnormalities. Ventricle size, however, is not represented in the polar map. By digitally subtracting the stress polar map from the rest polar map, the presence, extent and location of stress-induced perfusion defects are easily reviewed. It is critical that the rest and stress polar maps are based on identical delineation and orientation of the left ventricle. Otherwise, the corresponding parts of the polar maps do not relate to identical parts of the myocardium and serious falsely positive differences in perfusion may be presented in the polar maps. It should be emphasised that the polar map does not disclose possible artefacts such as extra-cardiac hot spots or attenuation problems.

*Three-dimensional display.* of the left ventricle may also facilitate assessment of the presence, extent and location of perfusion abnormalities. Ventricular size and configuration can be displayed. In addition it may be helpful for correlation of perfusion data with other examinations such as echocardiography and coronary angiography, in particular in the communication with clinical cardiologists.

#### Perfusion defects

An area of diminished uptake of the radiopharmaceutical has to be described with respect to localisation, severity and extent. If using a segmental model, the 17-segment model and the associated nomenclature is recommended, as this model provides the best agreement with other imaging modalities such as MRI, echocardiography and anatomical data [92].

The distribution of tracer uptake may be characterised visually [93, 94] as:

- Normal:  $\geq 70\%$
- Mildly reduced: 69–50%
- Moderately reduced: 49–30%
- Severely reduced: 29–10%
- Absent:  $< 10\%$

These figures refer to the activity distribution in healthy, gender-stratified, reference populations for the same LV region, which allows for the normal variation of count rates, e.g. septal count rate to be lower than that in the lateral wall in healthy subjects.

The extent of a perfusion abnormality can be qualified as small, intermediate or large.

#### Left ventricular size and function

A visual assessment of the LV cavity should be performed. With gated studies, quantitative measurements of volumes can be acquired (see Sect. “[Quantitative analysis](#)”).

Wall motion is reviewed without computer-derived edges. Computer-generated contours can be helpful, for

example with a fixed end-diastolic or end-systolic contour displayed on the cine images. Wall motion is classified as:

- Normal
- Hypokinetic
- Akinetic
- Dyskinetic (paradoxical)

Wall thickening is based on the increase in counts per pixel between diastole and systole and is therefore best visualised in a continuous colour display. Thickening is classified as normal, reduced or absent.

### *Quantitative analysis*

#### Regional myocardial perfusion

True quantification of regional myocardial perfusion is possible with PET, but not with SPECT, although several attempts are underway to create such programs for SPECT. Quantitative analysis of relative perfusion distribution and myocardial function is available and adds useful information, including prognostic information, thereby improving both reliability and reproducibility of interpretations. A number of programs for quantitative analysis have been validated. It is, however, important to emphasise that the quantitative analysis should be used as a supplement to the visual review of the images and should not be reported in isolation from the review of the images. Technical problems and most artefacts will not be recognised if only quantitative analysis is performed.

Some programs include manual steps such as identification of apex and base in the short axis slices of the rest and stress studies, resulting in considerable inter-operator variability. Completely automated programs have the advantage of low inter-operator variability, but there can be considerable differences between different automated programs quantifying perfusion defects, ventricular volumes or EF in the images. Physicians should be aware of the variability that exists between different programs, especially if more than one program is used at the same site.

#### Perfusion defects

There are several programs that highlight regions with “significantly” reduced tracer uptake and quantify the extent and severity of perfusion defects. This type of analysis is based on a database comprising a reference population, often a combination of subjects with low likelihood of coronary artery disease or normal coronary angiography and patients with known coronary artery disease. There are many parameters that potentially influence myocardial perfusion images, e.g. gender, tracer, acquisition and processing protocols, patient position and AC. Both a suitably large database and similarity with the aforementioned parameters for the locally examined patient population are important for a reliable analysis. These conditions, however,

are not always met, and the physician should be aware of this limitation, as well as the fact that small activity defects are often also found in healthy subjects.

*Segmental models.* One approach to quantify myocardial perfusion images is to first divide the myocardium into a number of segments, e.g. 17. Each segment is scored separately using a 5-point model ranging from 0 (normal uptake) to 4 (uptake absent). The total score of the left ventricle is referred to as the summed stress score (SSS), summed rest score (SRS) and summed difference score (SDS) [95, 96]. All scores have been shown to be of prognostic value (Fig. 10).

*Coronary artery supply and SPECT images.* Some quantitative analysis programs may offer the option of assigning myocardial segments to a specific vascular territory. One has to bear in mind, however, that there is a large inter-individual variability in the territories subtended by the three main coronary arteries and their branches. Programs that allow matching of the angiographic data and perfusion data within one person are not yet commercially available. Until they are, one will have to be careful in assigning myocardial segments to specific vascular territories.

*Pixel- and voxel-based models.* A quantitative analysis can be performed of the polar maps. Pixels with relative count values below reference limits are highlighted as black-outs. The number of pixels in the different vascular territories are calculated to give a quantification of the extent of a perfusion defects. There are also programs that use a three-dimensional analysis instead of the polar maps. In these programs, abnormal voxels are highlighted in the display and quantification of the perfusion defects is performed in a similar way.

#### Left ventricular size and function

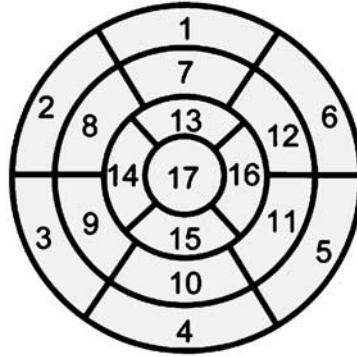
##### *Transient left ventricular cavity dilatation*

Transient LV cavity dilatation during stress has been shown to be a marker of coronary artery disease and an independent predictor of cardiac events [97, 98]. Automatic assessment of the transient ischaemic dilatation ratio is included in many of the software packages and this can be used as a complement to qualitative assessment of the cavity size in the rest and stress images.

##### *Left ventricular volumes, wall motion and wall thickening*

There are several commercially available programs for analysis of gated studies. LV end-diastolic volume, end-systolic volume, EF, regional wall motion and wall thickening (cf. Sect. “[Gated myocardial perfusion imaging](#)”) are generally presented by these programs. The results are based on computer-derived endocardial and epicardial edges. They should be reviewed for edge detection errors. Common sources of detection errors are: large myocardial

## a Left Ventricular Segmentation



- |                        |                       |                     |
|------------------------|-----------------------|---------------------|
| 1. basal anterior      | 7. mid anterior       | 13. apical anterior |
| 2. basal anteroseptal  | 8. mid anteroseptal   | 14. apical septal   |
| 3. basal inferoseptal  | 9. mid inferoseptal   | 15. apical inferior |
| 4. basal inferior      | 10. mid inferior      | 16. apical lateral  |
| 5. basal inferolateral | 11. mid inferolateral | 17. apex            |
| 6. basal anterolateral | 12. mid anterolateral |                     |

## b Coronary Artery Territories

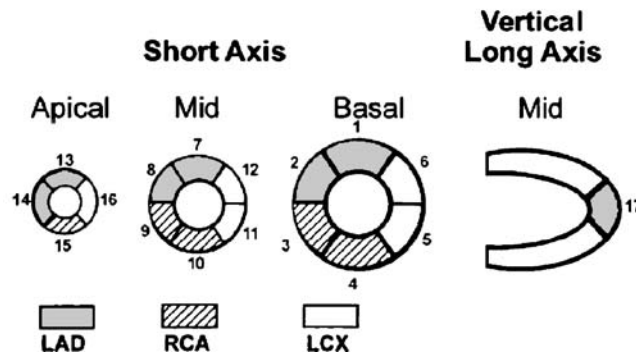


**Fig. 10. a** Segmentation of the polar plot format. Display, on a circumferential polar plot, of the 17 myocardial segments and the recommended nomenclature for tomographic imaging of the heart. **b** Seventeen-segment model and coronary artery territories. Assignment of the 17 myocardial segments to the territories of the left

anterior descending (*LAD*), right coronary artery (*RCA*) and left circumflex coronary artery (*LCX*). The large inter-individual variability in the territories subtended by the three main coronary arteries and their branches is emphasised: cf. the paragraph on coronary artery supply and SPECT images (modified from [121])

perfusion defects, extra-cardiac activity, small left ventricles, LV hypertrophy and images with low counts.

The accuracy of volume calculations has been well validated with MRI and contrast ventriculography as gold standards [99–102] for  $^{99m}\text{Tc}$ -labelled tracers, and to some degree also for  $^{201}\text{Tl}$ , which is less accurate for this purpose. The accuracy of regional systolic wall motion and thickening is less well validated and reference values limited.

### Integration of perfusion and function

Mild reduction of regional tracer uptake may represent a mild perfusion abnormality or an attenuation artefact. Information on wall motion and wall thickening in these regions may help to differentiate between these possibilities [71]. However, presence of regional wall motion and/or thickening does not exclude a stress-induced perfusion defect with the  $^{99m}\text{Tc}$  tracers, since the imaging is a re-

flection of post-stress myocardial function. Moreover, LV function has been shown to be an independent prognostic marker for cardiac events. The combined assessment of perfusion and function has major prognostic implications [103].

### Viability assessment

Myocardial viability is unlikely if regional tracer uptake is absent, and very likely if tracer uptake is similar to that in segments with normal function. Segments with uptake of at least 55% of peak activity and with detectable wall thickening have a high likelihood of functional recovery after revascularisation [104]. Lack of true rest in patients with coronary artery disease or incomplete redistribution of  $^{201}\text{Tl}$  may lead to underestimation of myocardial viability. In order to increase the correspondence of the resting images with myocardial viability, nitroglycerin adminis-

tration before injection of tracer at rest has been recommended [105, 106]. Viability assessment has been well documented by PET studies (cf. Sect. “[Positron emission tomography](#)”), but comparisons of combined  $^{18}\text{F}$ -FDG and perfusion SPECT with true PET examinations are very limited.

## 12. Reports, image display

### Reports

Reports should be typed and sent out promptly after the examination. They should be concise and couched in language that is easily understandable to referring physicians. The components discussed below should be considered as standard [45, 107, 108]. A summary is given in Table 18.

### Patient details and indication for study

The patient’s personal details (name, age, date of birth and gender) should be included at the start of the report. Any hospital/clinic identification number and the source of the referral should also be included. The clinical indication(s) for the study should be stated, including relevant clinical history. This will vary from patient to patient but may include symptoms, important cardiac events (recorded in chronological order), risk factors for coronary artery disease, the appearance of the resting electrocardiogram, and relevant details of prior diagnostic testing or intervention. The information provided in this section supports justification of the study and focusses the final conclusion.

### Stress technique and imaging protocol

The stress technique should be described briefly. For pharmacological stress, the agent and infusion protocol should be reported. Where dynamic exercise is used, the protocol together with exercise duration and/or maximal work load are relevant. Symptoms, haemodynamic changes, details of ECG changes during or after stress and current anti-anginal medication should be recorded irrespective of stress technique.

The imaging protocol should be specified, including the radiopharmaceutical used, type of stress study, imaging technique, sequence and date(s) of study.

### Findings

The appearance of the stress, rest and gated images should be described succinctly, including a statement on quality if suboptimal. Perfusion defects should be classified in terms of location relative to myocardial walls, extent and severity, and whether they are fixed, partially reversible or completely reversible. Common practice is to report the defect (s) in the stress tomograms in decreasing order of severity, and then to state how each defect changes in the rest tomograms in the same order. At this stage tracer uptake is being described.

Other abnormalities that should be mentioned are LV dilatation (persistent or transient), increased lung uptake of tracer, right ventricular uptake or significant non-cardiopulmonary tracer uptake.

Where ECG gated data are available, LVEF and volumes should be reported together with a description of regional myocardial wall motion and thickening. Caution should be exercised in reporting apparently spurious values of these parameters [109].

**Table 18.** Summary of recommendations for reporting

	Key points
Patient details	Name, age, gender, hospital identification number and date(s) of study
Indication(s) for study	Relevant data from medical history
Stress technique	Stress protocol: exercise type and maximal load and/or pharmacological stress agent and infused amount Response to stress: heart rate, systolic blood pressure, ECG changes, symptoms and adverse events (duration and intervention done)
Tracer and imaging protocol	Imaging protocol, including radiopharmaceutical and injected activities
Findings	Myocardial perfusion: presence, extent and depth of stress and rest defect(s), incl. information from gated images Pathology outside left ventricle: right ventricular visualisation, lung uptake, extracardiac focal accumulation Suboptimal image quality, significant artefact is present, if relevant
Conclusions	LV perfusion: inducible ischaemia (reversible perfusion defect); myocardial infarction (irreversible or permanent perfusion defect) LV function: global and regional function, possible stress-induced abnormalities Inconclusive study—may occasionally be the correct conclusion Correlation with and deviations from clinical information and other data if available. If clinically relevant: myocardial viability (hibernation, stunning), prognosis/risk assessment

## Conclusion

The findings should be integrated with the clinical data to reach a final interpretation [110]. A comparison with any previous study should be included.

It should be ensured that the conclusion answers the clinical question that prompted the referral if possible; if this is not possible, it may be relevant to make recommendations for further investigation or management.

- *Normal studies.* If the study is assessed to be normal, this should be stated, specifically bearing in mind that homogeneous myocardial perfusion during stress does not exclude non-obstructive coronary disease. The benign prognosis conferred by such a study should be stated.
- *Abnormal studies.* If the study is abnormal, the report should comment on the presence (if any) of inducible perfusion abnormality, infarction and significant artefact. If there is an abnormality, its location (in terms of segments affected), extent (in terms of numbers of segments affected) and severity should be noted. A statement on the likelihood of future coronary events may also be clinically relevant. This is deduced from the presence, extent and depth of inducible perfusion abnormalities, the LVEF if known, and other markers of prognosis such as transient dilatation and lung uptake. If no inducible perfusion abnormalities are present, then the EF is the main determinant of prognosis. The statement may be made in semi-quantitative terms (e.g. the likelihood of future coronary events is in the region of 5–10% per year) since the qualitative terms high, intermediate and low are not uniformly interpreted. High-risk patterns should be underscored.
- If correlation with coronary anatomy or assessment of myocardial viability or hibernation is relevant, this should be commented on, bearing in mind the normal variation of coronary anatomy.
- *Suboptimal quality of the study.* Where the study is suboptimal because of either an insufficient heart rate response during cardiac stress or technical problems during data acquisition, this should be stated and interpretation guarded. A recommendation to repeat the study using a different stress protocol or perfusion tracer, or increased injected activity, may be appropriate.

The information given above is summarised in Table 18.

### Image display

A hard copy of the images should accompany the report. All three projections in the standard orientation should be represented with careful alignment of the stress and rest slices (Fig. 11). If multiple slices are presented then short axis slices should be displayed with the apical slices to the far left and progression of slices toward the base in a left to right fashion, vertical long axis slices should be displayed

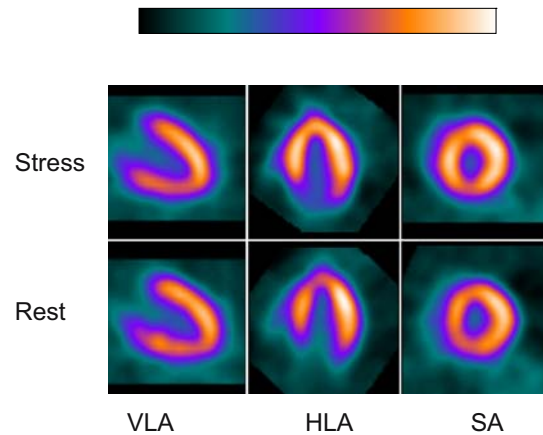


**Fig. 11.** Display of rest and stress studies in the three standard projections (example with GE colour scale), selected to illustrate the message of the report. *VLA* vertical long axis, *HLA* horizontal long axis, *SA* short axis

left to right from the septal slices through the midventricular slices to the lateral slices. and horizontal long axis slices should proceed left to right from the inferior to the anterior/superior surface (Fig. 12). It is important that the image set as a whole should be consistent with the image description [92, 111].

Stress and rest images should be presented in a format that allows ready comparison of corresponding tomograms, such as interactive displays that triangulate the three planes or display the full set of tomograms. Neighbouring pairs of tomograms can be summed for display according to local preference. Polar map displays can be a useful adjunct providing they are consistent with the tomograms and the report conclusion; they should not be provided in lieu of conventional displays.

Experts generally recommend that images be displayed using a continuous colour scale which should be shown on all image reproductions [112]. Each set of tomograms should be displayed with the top of the colour scale at the maximum within the myocardium for each set. Displays with the top of the colour scale at the maximum for each individual tomogram and those that use the same maximum for stress and rest images should not be used. Care should be taken if the maximum lies outside the myocardium or in different myocardial locations between stress and rest studies; these are cases where manual adjustment or masking of extracardiac activity may be required. The bottom end of the colour scale should be set to zero and background subtraction should be avoided.

Where an ECG-gated acquisition has been performed, the image display may include details of LV volumes and EF and polar maps of wall motion and wall thickening in addition to the tomograms. Regional wall motion is best displayed in a black and white scale, and wall thickening in a continuous colour scale (cf. Sect. “Gated myocardial perfusion imaging”).

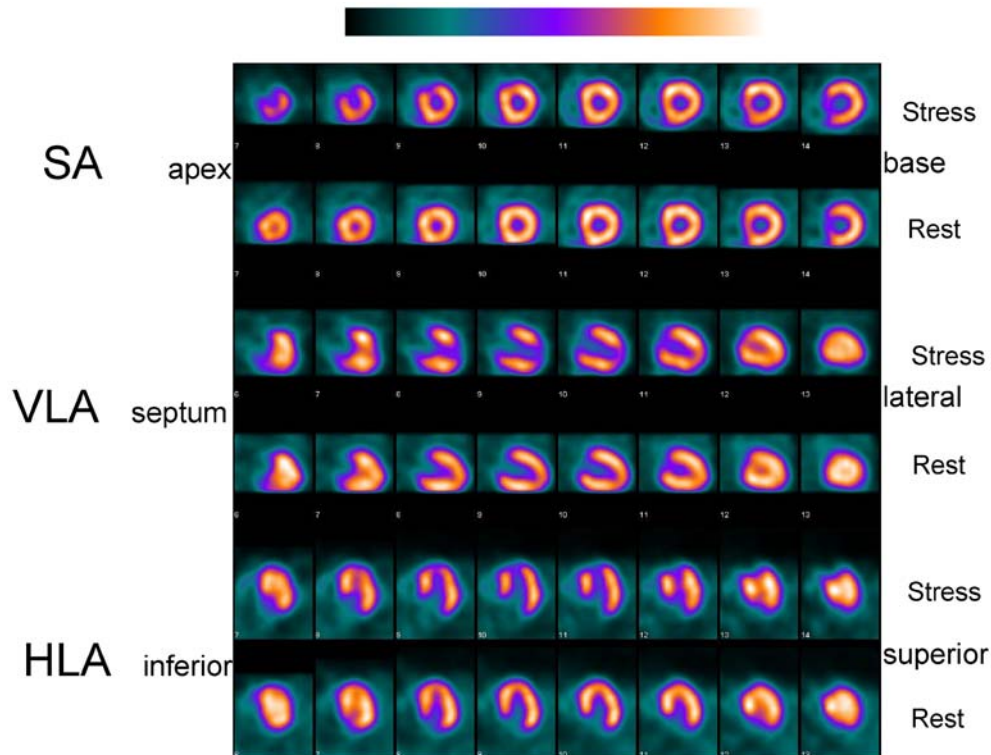


**Fig. 12.** Display of the stress and rest studies with all slices in the three standard projections: short axis (SA) from apex to base, vertical long axis (VLA) from septum to the lateral wall, and horizontal long axis (HLA) from the inferior to the anterior/superior wall

### 13. Positron emission tomography

Clinical cardiac PET imaging is performed for the assessment of myocardial perfusion and/or viability. The PET tracers used in clinical cardiac studies (Table 19) include different perfusion tracers, most often used in combination with the metabolic tracer  $^{18}\text{F}$ -FDG for viability studies.

The purpose of PET perfusion imaging at rest and during pharmacologic stress may be:

- Detection of myocardial ischaemia and/or infarction in patients with suspected or known coronary artery disease

- Determination of the extent and severity of disease
- Determination of individual risk for cardiac events, which serves to guide further workup.

Relative regional perfusion abnormalities are assessed in a manner similar to that in SPECT perfusion imaging, using  $^{13}\text{N}$ -ammonia or  $^{82}\text{Rb}$ . The usefulness of  $^{15}\text{O}$ -water as a freely diffusible tracer in this regard is less well documented.

In addition to regional assessment, all tracers allow for quantification of global myocardial blood flow and flow reserve. The usefulness of absolute flow measurements by PET has mainly been demonstrated for:

**Table 19.** Tracers for clinical cardiac PET

	$^{13}\text{N}$ -ammonia	$^{15}\text{O}$ -water	$^{82}\text{Rb}$	$^{18}\text{F}$ -FDG
Radioactive half-life	10 min	2 min	1.25 min	110 min
Recommended activity (MBq)	370–740	700–1,500	1,100–1,500 (–2,200)	200–350
Purpose	Myocardial perfusion			Myocardial viability
Advantages	Best PET image quality for myocardial perfusion. Quantification possible	Short half-life allows short protocols. Quantification possible	Generator-produced tracer	Combined with perfusion imaging unique in detection of tissue viability
Limitations	Half-life of 10 min extends duration of protocols	Does not produce perfusion images without dynamic modelling	Potassium analogue, suboptimal image quality	Uptake depends on metabolic environment

- Detection of microcirculatory impairment
- Determination of effects of therapeutic and preventive approaches in early stages of coronary disease

Myocardial metabolic imaging using  $^{18}\text{F}$ -FDG is the most frequent clinical application of cardiac PET. It is performed in patients with dysfunctional, hypoperfused myocardial regions to determine the likelihood of benefit from revascularisation. Residual metabolic activity is an indicator of myocardial viability, and thus of reversibility of contractile dysfunction. Increased regional FDG uptake relative to myocardial perfusion (perfusion/metabolism mismatch) indicates viability, whereas regional reduction of FDG uptake in proportion to perfusion (perfusion/metabolism match) indicates irreversibly damaged myocardium.

Myocardial FDG uptake can be imaged by SPECT using ultra-high-energy collimators. In this case, methodological issues specific to SPECT need to be considered for image interpretation. This also pertains to combinations of SPECT perfusion imaging and FDG PET imaging for viability assessment.

Clinical cardiac PET has been available for a relatively short time, and the techniques have been under rapid development. Furthermore, studies reported in the literature include only small samples of the very sick patients who are typical candidates for cardiac PET. The recommendations given below are therefore generally less evidence based than those for SPECT studies.

### Patient preparation

#### Perfusion studies

Perfusion measurements are often used clinically combined with FDG in the determination of viability. The subjects need no other preparation than that for FDG studies (cf. below). If a study is done on a separate day, overnight fasting (>6 h) is preferred. Alcohol and smoking should be discontinued for at least 12 h.

If adenosine or dipyridamole is used, caffeine-containing beverages, foods and medications should be discontinued (cf. Sect. “Stress tests” and Table 6).

#### $^{18}\text{F}$ -FDG studies

Myocardial FDG uptake depends on glucose and insulin plasma concentrations and the rate of glucose utilisation. Glucose uptake in peripheral tissues is the most important mechanism of clearance of FDG from the blood. High plasma glucose concentrations degrade the quality of the myocardial FDG uptake image. Myocardial FDG uptake is enhanced by factors increasing regional glucose utilisation such as increase in myocardial work, insulin and decrease in plasma levels of free fatty acids. It is necessary to standardise the metabolic environment for myocardial FDG imaging [113]. Three alternative methods are available to

**Table 20.** Acipimox and glucose loading protocols for FDG imaging in glucose-tolerant patients

Minute	Acipimox	Glucose loading
0	Patient arrives Measure blood (B-) glucose. If >7 mmol/l (>120 mg/dl), see Table 21 250 mg acipimox 500 mg acetosalicylic acid	Oral glucose 1 g/kg body wt.
60	250 mg acipimox	FDG 200–350 MBq
120	FDG 200–350 MBq	PET static image (15 min)
160	PET static image (15 min)	

improve myocardial FDG PET image quality: oral glucose loading, euglycaemic–hyperinsulinaemic clamping and the nicotinic acid derivative method (Tables 20, 21).

*Oral glucose loading.* Oral glucose loading (50–75 g) is the most common method. However, diagnostically unsatisfactory images may be obtained in 20–25% of patients with coronary artery disease [114, 115]. Abnormal glucose handling or type 2 diabetes, frequently undetected, may account for poor image quality in many of these patients.

*Insulin clamp.* Insulin clamping stimulates uptake of both glucose and FDG in the myocardium and in skeletal muscle and yields images of consistently high diagnostic quality,

**Table 21.** Acipimox protocol<sup>a</sup> for FDG imaging in diabetic patients and patients with glucose intolerance

Min	Acipimox	
0	Patient arrives Measure B-glucose. If <7 mmol/l (<120 mg/dl), see Table 20 250 mg acipimox 500 mg acetosalicylic acid	
60	250 mg acipimox	If B-glucose >7 mmol/l: 7–8 mmol/l (120–160 mg/dl) 2 units 8–10 mmol/l (161–180 mg/dl) 3 units >10 mmol/l (>180 mg/dl) 5 units
115	Measure B-glucose	
120	FDG 200–350 MBq	If B-glucose >7 mmol/l: Insulin 2–10 IU i.m., cf. above
160	PET static image (15 min)	If image quality is suboptimal, 2–5 IU insulin may be given i.v. and PET imaging repeated 60 min later, with monitoring of B-glucose at 15- to 30-min intervals
175	Meal, measure B-glucose	

<sup>a</sup>If the described nicotinic acid derivative method is used and insulin is also given, but the B-glucose concentration remains >7 mmol/l, one may switch to the insulin clamp method (clamp protocol not described in the present guidelines)

even in patients with diabetes. The clamp protocol is not described in the present guidelines.

*Nicotinic acid derivatives.* Nicotinic acid or its derivatives such as acipimox are effective for improving FDG image quality, and when combined with subcutaneous or intravenous injection of small amounts of short-acting insulin, good image quality can also be obtained in diabetic subjects [116–118]. With the exception of flushing, no side-effects of acipimox have been observed.

### Selection of technique

#### Patient preparation re glucose metabolism

*Non-diabetic patients.* In non-diabetic subjects, oral glucose loading and the nicotinic acid derivative method are both feasible, although the latter may give better image quality.

*Diabetic patients and patients with plasma glucose higher than 7 mmol/l.* Patients with abnormal glucose handling or diabetes represent a substantial fraction of those patients referred for assessment of myocardial viability. FDG images of poor quality are frequently obtained in these patients.

In diabetic patients or those with plasma glucose higher than 7 mmol/l (>120 mg/dl), the nicotinic acid derivative method [117] or euglycaemic–hyperinsulinaemic clamping can be used. Glucose loading is not recommended. At least 6 h of fasting is recommended before the start of the protocols. If B-glucose remains >7 mmol/l despite injection of small amounts of short-acting insulin, insulin clamp should be performed [119].

*Tracers and activities injected; image acquisition.* The supine position is preferred in the PET scanner with the arms out of the field of view. In the few cases where this is not possible (e.g. owing to severe arthritis), the arms can be within the field of view but it is critical to prevent them from moving between transmission and emission. When performing perfusion and metabolism studies, patient positioning should be identical in both studies. Correct positioning of the heart within the axial field of view of the tomograph may be ascertained by a scout scan, e.g. from a rectilinear transmission scan, if available. The transmission scan can be done either immediately before the emission scan or some minutes after an emission scan, when the radioactivity within the field of view is fairly stable.

- <sup>13</sup>N-ammonia The injected activity of <sup>13</sup>N-ammonia is typically 370–740 MBq (the amount is somewhat dependent on the sensitivity of the scanner), given as a bolus or short (<30 s) infusion. For viability studies, static imaging is started 1.5–3 min after the end of infusion and continued for 5–15 min. The attenuation-corrected images are reconstructed with a 2- to 3-mm

pixel size using standard FBP or an iterative reconstruction method. ECG-gated acquisition is optional.

- <sup>15</sup>O-water An activity of 700–1,500 MBq <sup>15</sup>O-water is injected as an intravenous bolus over 20–30 s. The activity to be injected depends on the PET camera system. Acquisition of the serial transaxial tomographic images of the heart is started (12 10-s frames, four 30-s frames and one 60-s frame, 5 min altogether). For repeated studies, 10-min intervals are recommended for radioactive decay between the flow measurements. Similar image reconstruction is performed as described above for <sup>13</sup>N-ammonia.
- Rubidium-82 The activity injected of <sup>82</sup>Rb is commonly 1,100–1,500 MBq, but in some PET systems higher activities are used (1,500–2,200 MBq). The tracer is injected as a bolus within 30 s or less and imaging time is 3–6 min, starting 70 s post injection (LVEF >50%) or 130 s post injection (LVEF <50%). The image reconstruction is similar to that when using <sup>13</sup>N-ammonia, as described above, except for reconstruction filtering (a Butterworth or low-pass filter 10- to 15-mm kernel is recommended; band pass filters are not recommended).
- <sup>18</sup>F-FDG The injected activity of <sup>18</sup>F-FDG is 200–350 MBq. Imaging is started 45–60 min post injection (the same for repeated studies) and image duration is 10–30 min (depending on count rate and dose). Currently 2D static acquisition is used but 3D or dynamic acquisition is optional if available. Similar image reconstruction is performed as with <sup>13</sup>N-ammonia. Gating: if wall motion information is useful, FDG gives higher image quality than perfusion images.

### Artefacts

Prior to interpretation and reporting, cardiac PET studies need to be reviewed for technical sources of error (Table 22). Retrospective detection of motion by analysis of images is often difficult (review of a projection movie, as done for SPECT studies, is not feasible for PET projections, which are all acquired simultaneously). Patient motion and transmission/emission misalignment can be identified by viewing non-reoriented transaxial images or sinograms. Special attention to patient position, which can be monitored using laser beams and skin markers, is important during acquisition of the study.

### Interpretation

#### Perfusion studies

Interpretation of LV myocardial perfusion is visually done by describing the extent, severity and location of perfusion defects at rest and, if acquired, during vasodilatation, along with their reversibility.

The extent and severity of perfusion defects may be assessed by:

**Table 22.** Technical errors in imaging

Error sources	Consequences
Patient motion during the acquisition of a perfusion or an FDG study	Blurring of contours
Patient motion between emission and transmission scans	Misalignment which may cause substantial changes in regional myocardial radioactivity following attenuation correction [120]
Patient motion between the acquisition of the perfusion and the FDG study	Misalignment, see above Risk of “false mismatch” if some of the well-perfused myocardium in the FDG study evaluation is thought to represent a region with hypoperfusion
Scattered coincidences from “hot” regions outside the myocardium	Artificially elevated regional count rates in adjacent myocardium
Errors in reconstruction algorithms	Artificially low count rates in areas close to extracardiac hot spots or areas

- *Semi-quantitative analysis*: a 17-segment model [121] has been suggested for semi-quantitative visual scoring and grading of the severity of defects (e.g. normal: 0, mild defect: 1, moderate defect: 2, severe defect: 3, absent uptake: 4). Scores of each segment can be summarised to derive summed stress, rest and difference scores (SSS, SRS, SDS) in a manner similar to SPECT imaging [121]. The normal heterogeneity for  $^{13}\text{N}$ -ammonia distribution with a mild reduction in lateral wall tracer uptake needs to be taken into account [122, 123]. No such heterogeneity has been reported for  $^{82}\text{Rb}$ .
- *Left ventricular polar maps*, which may be compared with normal databases to calculate extent of perfusion defects in % of left ventricle. In the literature, experience with visual and semi-quantitative perfusion analysis is mainly reported using  $^{13}\text{N}$ -ammonia or  $^{82}\text{Rb}$ , while very limited data exist for  $^{15}\text{O}$ -water.
- *Absolute quantification* of myocardial perfusion in ml/min/g tissue including flow reserve (hyperaemic flow/baseline flow), which is feasible and well established using dynamic image acquisition after injection of  $^{13}\text{N}$ -ammonia or  $^{15}\text{O}$ -water [124–128]. Some studies have also reported the feasibility of using  $^{82}\text{Rb}$  for absolute flow quantification [129], but theoretical limitations are obvious. Quantitative data can support visual and semiquantitative image interpretation, and may aid in assessing the physiological significance of known coronary stenoses [130, 131].

Quantitative assessment of perfusion may be helpful to detect balanced reduction of perfusion in multivessel disease and to identify an inadequate response to pharmacological vasodilation. A “perfusion threshold” for myocardial viability cannot be defined.

The evaluation of  $^{13}\text{N}$ -ammonia images should include an evaluation of structures outside the LV myocardium. Lung uptake of  $^{13}\text{N}$ -ammonia is occasionally seen, but no relation has been established between lung uptake of PET perfusion tracers and prognosis as in SPECT. Uptake in liver and intestine may be helpful for identification of artefacts. With  $^{82}\text{Rb}$  images, blood pool activity may be elevated

in the event of too early acquisition or prolonged tracer circulation times.

#### Viability studies

Evaluation of extracardiac structures should be part of the interpretation of cardiac FDG images, since focal FDG uptake may represent malignancy and/or inflammation. Blood pool activity also needs to be assessed, since it is inversely related to the quality of myocardial images. Increased FDG blood pool activity may be caused by inadequate patient preparation (high plasma free fatty acids, low plasma insulin), insulin resistance, diabetes or too early image acquisition. Repeat imaging after an additional 30–60 min is an option in such cases, as is the additional administration of short-acting insulin while monitoring blood glucose levels.

The goal of visual analysis is to identify fairly large hypokinetic or akinetic myocardial regions with a concomitant reduction in perfusion and metabolism (matched defect), indicating irreversibly damaged myocardium, regions with reduced perfusion but preserved or enhanced metabolism (perfusion/metabolism mismatch), indicating viable myocardium, and regions with normal perfusion, which are considered viable, indicating stunned myocardium (Table 23).

*Visual analysis.* For visual analysis of myocardial FDG uptake, it is helpful first to evaluate uptake in the myocardial segment with the highest perfusion. FDG uptake in other myocardial segments can then be evaluated relative to FDG uptake in those segments and compared with perfusion tracer uptake in the respective segments. Under insulin stimulation, myocardial FDG uptake is usually greatest in the regions with highest perfusion. FDG uptake in healthy myocardium may be higher in the lateral wall than the septum (uptake is especially pronounced under fasting conditions or little insulin stimulation) [132, 133]. Sometimes, a pattern of normal perfusion with reduced FDG uptake, “*reverse mismatch*”, is observed. In most cases it is related to inadequate normalisation of FDG

**Table 23.** Interpretation and reporting of viability studies

Myocardium	Wall motion	Perfusion	FDG uptake	Functional recovery after successful revascularisation
Normal	+	Normal	Normal	Not relevant
Scar	–	Reduced	Reduced	Not likely
Dysfunctional, but viable	–	Normal (“acute stunning”)	Normal or high	Probable, ± revascularisation
		Reduced (repetitive stunning, hibernation)	Normal or high	Probable

uptake, but it has also been described following PTCA or thrombolysis for acute myocardial infarction [134, 135]. Little is known about the clinical relevance of this pattern. Generally such areas are viable because perfusion is normal.

No attempt should be made to interpret images obtained under fasting conditions.

*Semi-quantitative analysis.* Semi-quantitative analysis can be done either using a visual segmental scoring system similar to that employed for perfusion studies or on the basis of a polar map. It should support the visual analysis. Currently there is little standardisation in the literature. A semi-quantitative approach, which should be validated at each lab, will increase study reproducibility and should permit an estimate of the extent of scar or mismatch in percentage of the left ventricle. This is important because the extent of mismatch, i.e. the amount of viable and non-viable tissue, has been shown to have a significant influence on the likelihood of recovery of global function following revascularisation [136–138].

*Quantitative analysis.* Absolute quantification of myocardial metabolic rate of glucose in  $\mu\text{mol}$  glucose/min/g tissue has been suggested [139, 140], but high inter-individual variability even under standardised conditions of euglycaemic–hyperinsulinaemic clamping limits its usefulness.

#### *ECG-gated perfusion and $^{18}\text{F}$ -FDG studies*

Gated PET acquisition can be performed at minimal expense, and some additional information may be obtained. If display and analysis follow a standardised approach, gated PET findings such as global LVEF and LV volumes can be included in the final report. Detection of regional contractile dysfunction may also be helpful to identify stunning in areas of preserved perfusion or to assess the

degree of residual viability in areas with mildly matched perfusion/metabolism defects. Further studies are necessary to establish the incremental value of gating of cardiac PET studies.

#### *The report*

The typical report is similar to that for myocardial perfusion SPECT (cf. Sect. “[Reports, image display](#)”). The question of viability is relevant only when there is regionally reduced contractility in a significant part of the left ventricle. Because patients submitted for viability imaging most often suffer from complex, advanced coronary artery disease, integration of all available angiographic and regional wall motion data is important for a final interpretation. The typical report includes:

- Patient-specific information
- Relevant history and key clinical findings
- Indication for the study
- Type of the study (radiopharmaceuticals, acquisition protocol, type of metabolic preparation), summary of dietary state and metabolic data, resting haemodynamics and ECG
- Image description (visual, semi-quantitative, quantitative evaluation of match/mismatch with description of extent of viable tissue)
- Conclusion

#### *Image display*

Cardiac perfusion and viability images generated by PET are typically displayed similarly to SPECT images after re-orientation along the short axis and vertical and horizontal long axes of the heart. If rest and stress perfusion and/or metabolism are determined during a single PET imaging session, and if the patient has not moved between acquisitions, the individually defined axes can be copied from one study to another for optimal regional matching. Additionally, software routines are available for calculation of LV polar maps (bull’s eye plots) to support visual analysis of re-oriented slices [122, 123, 141]. Since  $^{15}\text{O}$ -water does not produce automatically images of myocardial perfusion, it is recommended that  $^{13}\text{N}$ -ammonia or  $^{82}\text{Rb}$  is used as a perfusion tracer for viability studies, unless parametric images or polar maps can be created from  $^{15}\text{O}$ -water studies by setting the region with maximal tracer uptake to 100%. For interpretation of metabolic images, the images are best normalised to the region with the highest uptake of the perfusion tracer, because FDG uptake may be enhanced in regions of normal perfusion, e.g. as a consequence of post-ischaemic stunning.

The right ventricle should be evaluated with regard to size, hypertrophy and perfusion defects.

*SPECT for assessment of myocardial metabolism and/or perfusion*

If metabolic FDG PET studies are interpreted in combination with SPECT perfusion images, potential reduction of perfusion tracer uptake due to attenuation needs to be considered for relative comparison of perfusion and metabolism. The risk of false-positive diagnosis of mismatch due to an attenuation artefact in SPECT in a/hypokinetic regions may be reduced by AC of the SPECT images. SPECT perfusion is not recommended in patients with inferior wall akinesia, where the attenuation problems are most frequently observed.

If FDG images are acquired with a SPECT camera using a 511-keV collimator, additional problems may be encountered due to:

- Attenuation (which is less for 511 keV than for low-energy perfusion tracers, resulting in false positive mismatch)
- Lower spatial resolution compared with the low-energy collimators used for SPECT perfusion tracers (again, there is risk of false positive mismatch).

Polar map analysis using normal databases may overcome some of those problems.

*Acknowledgements.* We wish to thank the European Association of Nuclear Medicine for financial support. We thank the European Council of Nuclear Cardiology for support and national European societies of nuclear medicine and cardiology for helpful information. The group is grateful to Jenny Sandgren for her devoted efforts with secretarial assistance.

## References

1. Anagnostopoulos C, Harbinson M, Kelion A, Kundley K, Loong CY, Notghi A, et al. Procedure guidelines for radionuclide myocardial perfusion imaging. *Heart* 2004;90 Suppl 1:i1–10.
2. ESC Guidelines for exercise testing.
3. American guidelines (the ACC/AHA exercise testing guidelines).
4. Society of Nuclear Medicine procedure guideline for myocardial perfusion imaging.
5. American Society of Nuclear Cardiology: imaging guidelines for nuclear cardiology procedures.
6. Grunwald AM, Watson DD, Holzgrefe HH Jr, Irving JF, Beller GA. Myocardial thallium-201 kinetics in normal and ischaemic myocardium. *Circulation* 1981;64:610–8.
7. Ingwall JS, Kramer M, Kloner NM, et al. Thallium accumulation: differentiation between reversible and irreversible myocardial injury. *Circulation* 1979;59:678. (abstract).
8. Dilsizian V, Rocco TP, Freedman NM, Leon MB, Bonow RO. Enhanced detection of ischaemic but viable myocardium by the reinjection of thallium after stress-redistribution imaging. *N Engl J Med* 1990;323:141–6.
9. van Eck-Smit BL, van der Wall EE, Zwinderman AH, Pauwels EK. Clinical value of immediate thallium-201 reinjection imaging for the detection of ischaemic heart disease. *Eur Heart J* 1995;16:410–20.
10. Li QS, Solot G, Frank TL, Wagner HNJ, Becker LC. Myocardial redistribution of technetium-99m-methoxyisobutyl isonitrile (SESTAMIBI). *J Nucl Med* 1990;31:1069–76.
11. Jain D, Wackers FJ, Mattera J, McMahon M, Sinusas AJ, Zaret BL. Biokinetics of technetium-99m-tetrofosmin: myocardial perfusion imaging agent: implications for a one-day imaging protocol. *J Nucl Med* 1993;34:1254–9.
12. Münch G, Neverve J, Matsunari I, Schröter G, Schwaiger M. Myocardial technetium-99m-tetrofosmin and technetium-99m-sestamibi kinetics in normal subjects and patients with coronary artery disease. *J Nucl Med* 1997;38:428–32.
13. Maurea S, Cuocolo A, Soricelli A, Castelli L, Nappi A, Squame F, et al. Enhanced detection of viable myocardium by technetium-99m-MIBI imaging after nitrate administration in chronic coronary artery disease. *J Nucl Med* 1995;36:1945–52.
14. Thorley PJ, Bloomer TN, Sheard KL, Sivananthan UM. The use of GTN to improve the detection of ischaemic myocardium using Tc-99m-tetrofosmin. *Nucl Med Commun* 1996;17:669–74.
15. Vanzetto G, Fagret D, Pasqualini R, Mathieu JP, Chossat F, Machecourt J. Biodistribution, dosimetry, and safety of myocardial perfusion imaging agent <sup>99m</sup>TcN-NOET in healthy volunteers. *J Nucl Med* 2000;41:141–8.
16. Cuocolo A, Rubini G, Acampa W, Nicolai E, Florimonte L, DiGiovine G, et al. Technetium 99m furifosmin regional myocardial uptake in patients with previous myocardial infarction: relation to thallium-201 activity and left ventricular function. *J Nucl Cardiol* 2000;7:235–41.
17. [CD97] Council Directive 97/43/Euratom of 30 June 1997 on health protection of individuals against the dangers of ionizing radiation in relation to medical exposure, and repealing Directive 84/466/Euratom. *Official J Eur Commun* 1997; L 180:22–7.
18. Heo J, Powers J, Iskandrian AE. Exercise–rest same-day SPECT sestamibi imaging to detect coronary artery disease. *J Nucl Med* 1997;38:200–3.
19. Garcia EV, Cooke CD, Van Train KF, Folks R, Peifer J, DePuey EG, et al. Technical aspects of myocardial SPECT imaging with technetium-99m sestamibi. *Am J Cardiol* 1990; 66:23E–31E.
20. ICRP Publication 80. Radiation dose to patients from radiopharmaceuticals. *Annals of ICRP*, 28. Oxford: Pergamon Press; 1998. p. 3.
21. ICRP Publication 53. Radiation dose to patients from radiopharmaceuticals. *Annals of ICRP*, 18. Oxford: Pergamon Press; 1987. p. 1–4.
22. ICRP Publication 60. 1990 Recommendations of the ICRP. *Annals of ICRP*, 21. Oxford: Pergamon Press; 1992. p. 1–3.
23. Piepsz A, Hahn K, Roca I, Ciofetta G, Toth G, Gordon I, et al. A radiopharmaceuticals schedule for imaging in paediatrics. Paediatric Task Group European Association Nuclear Medicine. *Eur J Nucl Med* 1990;17(3–4):127–9.
24. Strahlenschutzkommission. Strahlenexposition von Personen durch nuklearmedizinisch untersuchte Patienten. In: Gumprecht D, Heller H, editors. *Empfehlungen und Stellungnahmen der Strahlenschutzkommission* 1998, Bonn. 1999
25. Radiation Protection 100. Guidance for protection of unborn children and infants irradiated due to parental medical exposures. European Commission on-line publication catalogue 1998, <http://europa.eu.int/comm/environment/pubs/nuclear.htm#100>
26. Clinical competence statement on exercise stress testing. AHA/ACC Task Force Report. *J Am Coll Cardiol* 2000; 36:1441–53.

27. Guidelines for clinical use of cardiac radionuclide imaging. AHA/ACC Task Force Report. *Circulation* 1995;91:1278–1303.
28. Guidelines for exercise stress testing. AHA/ACC Task Force Report. *J Am Coll Cardiol* 1997;30:260–315.
29. Pennell DJ, Mavrogeni SI, Forbat SM, Karwatowski SP, Underwood SR. Adenosine combined with dynamic exercise for myocardial perfusion imaging. *J Am Coll Cardiol* 1995; 25:1300–9.
30. Samady H, Wackers FJ, Joska T, Zaret B, Jain D. Pharmacologic stress perfusion imaging with adenosine: role of simultaneous low-level treadmill exercise. *J Nucl Cardiol* 2002;9:188–96.
31. Thomas GS, Prill NV, Majmundar H, Fabrizi RR, Thomas JJ, Hayashida C, et al. Treadmill exercise during adenosine infusion is safe, results in fewer adverse reactions, and improves myocardial perfusion image quality. *J Nucl Cardiol* 2000;7:439–46.
32. Treuth MG, Reyes GA, He ZX, Cwajg E, Mahmarian JJ, Verani MS. Tolerance and diagnostic accuracy of an abbreviated adenosine infusion for myocardial scintigraphy: a randomized prospective study. *J Nucl Cardiol* 2001;8:548–54.
33. Cerqueira MD, Verani MS, Schwaiger M, Heo J, Iskandrian AS. Safety profile of adenosine stress perfusion imaging; results from the Adenoscan Multicenter Trial Registry. *J Am Coll Cardiol* 1994;23:384–90.
34. Lette J, Tatum JL, Fraser S, Miller DD, Waters DD, Heller G, et al. Safety of dipyridamole testing in 73,806 patients: the Multicenter Dipyridamole Safety study. *J Nucl Cardiol* 1994; 2:3–17.
35. McNeill AJ, Fioretti PM, el-Said SM, Salustri A, Forster T, Roelandt JR. Enhanced sensitivity for detection of coronary artery disease by addition of atropine to dobutamine stress echocardiography. *Am J Cardiol* 1992;70:41–6.
36. Hicks RJ. Myocardial perfusion scintigraphy techniques using single photon radiotracers. In: Murray E, editor. *Nuclear medicine in diagnosis and treatment*. 2nd ed. New York: Churchill Livingstone; 1998. p. 1333–51.
37. Rocco TP, Dilsizian V, McKusick KA, Fischman AJ, Boucher CA, Strauss HW. Comparison of thallium redistribution with rest “re-injection” imaging for detection of viable myocardium. *Am J Cardiol* 1990;66:158–63.
38. Heo J, Kegel J, Iskandrian AS, Cave V, Iskandrian BB. Comparison of same-day protocols using technetium-99m-sestamibi myocardial imaging. *J Nucl Med* 1992;33:186–91.
39. van Dongen AJ, van Rijk PP. Minimizing liver, bowel, and gastric activity in myocardial perfusion SPECT. *J Nucl Med* 2000;41:1315–7.
40. Hurwitz GA, Clark EM, Slomka PJ, Siddiq SK. Investigation of measures to reduce interfering abdominal activity on rest myocardial images with Tc-99m sestamibi. *Clin Nucl Med* 1993;18:735–41.
41. Berman DS, Kiat HS, Van Train KF, Germano G, Maddahi J, Friedman JD. Myocardial perfusion imaging with technetium-99m-sestamibi: comparative analysis of available imaging protocols. *J Nucl Med* 1994;35 4:681–8.
42. Segall GM, Davis MJ. Prone versus supine thallium myocardial SPECT: a method to decrease artefactual inferior wall defects. *J Nucl Med* 1989;30:548–55.
43. Strauss HW, Miller DD, Wittry MD, Cerqueira MD, Garcia EV, Iskandrian AS, et al. Procedure guideline for myocardial perfusion imaging. Society of Nuclear Medicine. *J Nucl Med* 1998;39:918–23.
44. Eisner RL, Nowak DJ, Pettigrew R, Fajman W. Fundamentals of 180-degree acquisition and reconstruction in SPECT imaging. *J Nucl Med* 1986;27:1717–28.
45. DePuey EG, Garcia E, Borges-Neto S, Jain D, Fiacro E, Nichols K, et al. Updated imaging guidelines for nuclear cardiology procedures, part 1. *J Nucl Cardiol* 2001;8:G1–58.
46. IAEA TECDOC-602. Quality control of nuclear medicine instruments 1991. ISSN 1011–4289, International Atomic Energy Agency, Vienna.
47. Society of nuclear medicine procedure guideline for general imaging, version 2.0. Society of Nuclear Medicine (<http://www.snm.org>), 1999.
48. Report 86 Quality control of gamma camera systems In: Bolster A, editor. *Institute of Physics in Engineering and Medicine*, 2003. ISBN 1 903613 13 2.
49. O'Connor MK, Hung JCY. Instrumentation quality control. In: O'Connor MK, editor. *Mayo Clinic manual of nuclear medicine*. New York: Churchill Livingstone; 1996. p. 1–57.
50. IAEA quality control atlas for scintillation systems (compiler/author: E. Busemann Sokole). ISBN 92-0-101303-5. International Atomic Energy Agency, Vienna, 2003.
51. NEMA NU1-2001 Performance measurements of scintillation cameras. Standards publication, National Electrical Manufacturer's Association, 2001.
52. Busemann Sokole E. Measurement of collimator hole angulation and camera head tilt for slant and parallel hole collimators used in SPECT. *J Nucl Med* 1987;28:1592–8.
53. Bracewell RN, Riddle AC. Inversion of fan-beam scans in radioastronomy. *Astrophys J* 1967;150:427–38.
54. Hutton BF, Hudson HM, Beekman FJ. A clinical perspective of accelerated statistical reconstruction. *Eur J Nucl Med* 1997;24:797–808.
55. Hudson HM, Larkin RS. Accelerated image reconstruction using ordered subsets of projection data. *IEEE Trans Nucl Sci* 1994;41:1360–9.
56. Llacer J, Velkerov E. Feasible images and practical stopping rules for iterative algorithms in emission tomography. *IEEE Trans Med Imag* 1989;8:186–93.
57. Butterworth S. On the theory of filter amplifiers. *Exp Wirel Wirel Eng* 1930;7:536–41.
58. Links JM, Jeremy RW, Dyer SM, Frank TL, Becker LC. Wiener filtering improves quantification of regional myocardial perfusion with thallium-201 SPECT. *J Nucl Med* 1990;31:1230–6.
59. Miller TR, Sampathkumaran KS. Design and application of finite impulse response digital filters. *Eur J Nucl Med* 1982; 7:22–7.
60. Germano G, Chua T, Kavanagh PB, Kiat H, Berman DS. Detection and correction of patient motion in dynamic and static myocardial SPECT using a multi-detector camera. *J Nucl Med* 1993;34:1349–55.
61. Matsumoto N, Berman DS, Kavanagh PB, Gerlach J, Hayes SW, Lewin HC, et al. Quantitative assessment of motion artifacts and validation of a new motion-correction program for myocardial perfusion SPECT. *J Nucl Med* 2001;42:687–94.
62. Friedman J, Van Train K, Maddahi J, Rozanski A, Prigent F, Bietendorf J, et al. “Upward creep” of the heart: a frequent source of false-positive reversible defects during thallium-201 stress-redistribution SPECT. *J Nucl Med* 1989;30:1718–22.
63. DePuey EG, Garcia EV. Optimal specificity of thallium-201 SPECT through recognition of imaging artifacts. *J Nucl Med* 1989;30:441–9.

64. Germano G, Kavanagh PB, Chen J, Waechter P, Su HT, Kiat H, et al. Operator-less processing of myocardial perfusion SPECT studies. *J Nucl Med* 1995;36:2127–32.
65. Slomka PJ, Hurwitz GA, Stephenson J, Craddock T. Automated alignment and sizing of myocardial stress and rest scans to three-dimensional normal templates using an image registration algorithm. *J Nucl Med* 1995;36:1115–22.
66. Choi JY, Lee KH, Kim SJ, Kim SE, Kim BT, Lee SH, et al. Gating provides improved accuracy for differentiating artifacts from true lesions in equivocal fixed defects on technetium 99m tetrofosmin perfusion SPECT. *J Nucl Cardiol* 1998;5:395–401.
67. Germano G, Berman DS. Acquisition and processing for gated perfusion SPECT: technical aspects. In: Germano G, Berman DS, editors. *Clinical cardiac SPECT*. Armonk, NY: Futura Publishing Company; 1999. p. 93–113.
68. Manrique A, Faraggi M, Vera P, Vilain D, Lebtahi R, Cribier A, et al.  $^{201}\text{Tl}$  and  $^{99\text{m}}\text{Tc}$ -MIBI gated SPECT in patients with large perfusion defects and left ventricular dysfunction: comparison with equilibrium radionuclide angiography. *J Nucl Med* 1999;40:805–9.
69. De Puey EG, Parmett S, Ghesani M, Rozanski A, Nichols K, Salensky H. Comparison of Tc-99m sestamibi and Tl-201 gated perfusion SPECT. *J Nucl Cardiol* 1999;6:278–85.
70. Sharir T, Germano G, Kang X, Cohen I, Friedman JD, Berman DS. Prognostic value of post-stress left ventricular volume and ejection fraction by gated myocardial perfusion single photon emission computed tomography in women: gender related differences in normal limits and outcome. *Circulation* 2002;106(19):II-523. (abstract).
71. Smanio PE, Watson DD, Segalla DL, Vinson EL, Smith WH, Beller GA. Value of gating of technetium-99m sestamibi single-photon emission computed tomographic imaging. *J Am Coll Cardiol* 1997;30:1687–92.
72. Lima RS, Watson DD, Goode AR, Siadaty MS, Ragosta M, Beller GA, et al. Incremental value of combined perfusion and function over perfusion alone by gated SPECT myocardial perfusion imaging for detection of severe three-vessel coronary artery disease. *J Am Coll Cardiol* 2003;42:64–70.
73. Sharir T, Germano G, Kavanagh PB, Lai S, Cohen I, Lewin HC, et al. Incremental prognostic value of post-stress left ventricular ejection fraction and volume by gated myocardial perfusion single photon emission computed tomography. *Circulation* 1999;100:1035–42.
74. Ficaro E, Fessler J, Shreve P, Kritzman J, Rose P, Corbett J. Simultaneous transmission/emission myocardial perfusion tomography: diagnostic accuracy of attenuation-corrected Tc-99m sestamibi single-photon emission computed tomography. *Circulation* 1996;93:463–73.
75. Prvulovich EM, Lonn AH, Bomanji JB, Jarritt PH, Ell PJ. Effect of attenuation correction on myocardial thallium-201 distribution in patients with a low likelihood of coronary artery disease. *Eur J Nucl Med* 1997;24:266–75.
76. Kluge R, Sattler B, Seese A, Knapp WH. Attenuation correction by simultaneous emission–transmission myocardial single-photon emission tomography using technetium-99m labelled radiotracer: impact on diagnostic accuracy. *Eur J Nucl Med* 1997;24:1107–14.
77. Hendel RC, Berman DS, Cullom SJ, Follansbee W, Heller GV, Kiat H, et al. Multicenter clinical trial to evaluate the efficacy of correction for photon attenuation and scatter in SPECT myocardial perfusion imaging. *Circulation* 1999;99:2742–9.
78. Matsunari I, Boning G, Ziegler SI, Nekolla SG, Stollfuss JC, Kosa I, et al. Attenuation corrected Tc-99m-tetrofosmin single-photon emission computed tomography in the detection of viable myocardium: comparison with positron emission tomography using  $^{18}\text{F}$ -fluorodeoxyglucose. *J Am Coll Cardiol* 1998;32:927–35.
79. Chouraqui P, Livschitz S, Sharir T, Wainer N, Wilk M, Moalem I, et al. Evaluation of an attenuation correction method for thallium-201 myocardial perfusion tomographic imaging of patients with low likelihood of coronary artery disease. *J Nucl Cardiol* 1998;5:369–77.
80. Rigo P, Van Boxem P, Foulon J, Safi M, Engdahl J, Links J. Quantitative evaluation of a comprehensive motion, resolution, and attenuation correction program: initial experience. *J Nucl Cardiol* 1998;5:458–68.
81. Vidal R, Buvat I, Darcourt J, Migneco O, Desvignes P, Baudouy M, et al. Impact of attenuation correction by simultaneous emission/transmission tomography on visual assessment of  $^{201}\text{Tl}$  myocardial perfusion images. *J Nucl Med* 1999;40:1301–9.
82. Should SPET attenuation correction be more widely employed in routine clinical practice? For: Ficaro EP; Against: Wackers FJT. *Eur J Nucl Med Mol Imaging* 2002;29:409–15.
83. Hendel RC, Corbett JR, Cullom SJ, DePuey EG, Garcia EV, Bateman TM. The value and practice of attenuation correction for myocardial perfusion SPECT imaging: a joint position statement from the American Society of Nuclear Cardiology and the Society of Nuclear Medicine. *J Nucl Cardiol* 2002;9:135–43.
84. Corbett RJ, Ficaro EP. Clinical review of attenuation-corrected cardiac SPECT. *J Nucl Cardiol* 1999;6:54–68.
85. O'Connor MK, Kemp B, Anstett F, Christian P, Ficaro EP, Frey E, et al. A multicenter evaluation of commercial attenuation compensation techniques in cardiac SPECT using phantom models. *J Nucl Cardiol* 2002;9:361–76.
86. Zaidi H, Koral KF. Scatter modelling and compensation in emission tomography. *Eur J Nucl Med Mol Imaging* 2004;31:761–82.
87. Links JM, Becker LC, Rigo P, Taillefer R, Hanelin L, Anstett F, et al. Combined corrections for attenuation, depth-dependent blur, and motion in cardiac SPECT: a multicenter trial. *J Nucl Cardiol* 2000;7:414–25.
88. Narayanan MV, King MA, Pretorius PH, Dahlberg ST, Spencer F, Simon E, et al. Human-observer receiver-operating characteristic evaluation of attenuation, scatter, and resolution compensation strategies for  $^{99\text{m}}\text{Tc}$  myocardial perfusion imaging. *J Nucl Med* 2003;44:1725–34.
89. Wackers FJT. Attenuation compensation of cardiac SPECT: a critical look at a confusing world (editorial). *J Nucl Cardiol* 2002;9:438–40.
90. Gallowitsch HJ, Sykora J, Mikosch P, Kresnik E, Unterweger O, Molnar M, et al. Attenuation-corrected thallium-201 single-photon emission tomography using a gadolinium-153 moving line source: clinical value and the impact of attenuation correction on the extent and severity of perfusion abnormalities. *Eur J Nucl Med* 1998;25:220–8.
91. Almquist H, Arheden H, Arvidsson AH, Pahlm O, Palmer J. Clinical implication of down-scatter in attenuation-corrected myocardial SPECT. *J Nucl Cardiol* 1999;6:406–11.

92. Cerqueira MD, Weissman NJ, Dilsizian V, Jacobs AK, Kaul S, Laskey WK, et al. Standardized myocardial segmentation and nomenclature for tomographic imaging of the heart. A statement for healthcare professionals from the Cardiac Imaging Committee of the Council on Clinical Cardiology of the American Heart Association. *Circulation* 2002;105:539–42.
93. Shehata AR, Ahlberg AW, White MP, Russell A, Fleming IA, Levine MG, et al. Dipyridamole–dobutamine stress with Tc-99m sestamibi tomographic myocardial perfusion imaging. *Am J Cardiol* 1998;82:520–3.
94. Van Train KF, Alreeda J, Garcia EV, Cooke CD, Maddahi J, Kiat H, et al. Quantitative same-day rest–stress technetium-99m-sestamibi SPECT: definition and validation of stress normal limits and criteria for abnormality. *J Nucl Med* 1993;34:1494–502.
95. Berman DS, Kang X, Van Train KF, Lewin HC, Cohen I, Areeda J, et al. Comparative prognostic value of automatic quantitative analysis versus semiquantitative visual analysis of exercise myocardial perfusion single-photon emission computed tomography. *J Am Coll Cardiol* 1998;32:1987–95.
96. Sharir T, Berman DS, Waechter PB, Areeda J, Kavanagh PB, Gerlach J, et al. Quantitative analysis of regional motion and thickening by gated myocardial perfusion SPECT: normal heterogeneity and criteria for abnormality. *J Nucl Med* 2001;42:1630–8.
97. McClellan JR, Travin MI, Herman SD, Baron JJ, Golub RJ, Gallagher JJ, et al. Prognostic importance of scintigraphic left ventricular cavity dilation during intravenous dipyridamole technetium-99m sestamibi myocardial tomographic imaging in predicting coronary events. *Am J Cardiol* 1997;79:600–5.
98. Mazzanti M, Germano G, Kiat H, Kavanagh PB, Alexanderson E, Friedman JD, et al. Identification of severe and extensive coronary artery disease by automatic measurement of transient ischemic dilation of the left ventricle in dual-isotope myocardial perfusion SPECT. *J Am Coll Cardiol* 1996;27:1612–20.
99. Ioannidis JP, Trikalinos TA, Danias PG. Electrocardiogram-gated single-photon emission computed tomography versus cardiac magnetic resonance imaging for the assessment of left ventricular volumes and ejection fraction: a meta-analysis. *J Am Coll Cardiol* 2002;39:2059–68.
100. Tadamura E, Kudoh T, Motooka M, Inubushi M, Shirakawa S, Hattori N, et al. Assessment of regional and global left ventricular function by reinjection Tl-201 and rest Tc-99m sestamibi ECG-gated SPECT: comparison with three-dimensional magnetic resonance imaging. *J Am Coll Cardiol* 1999;33:991–7.
101. Bavelaar-Croon CD, Kayser HW, van der Wall EE, de Roos A, Dibbets-Schneider P, Pauwels EK, et al. Left ventricular function: correlation of quantitative gated SPECT and MR imaging over a wide range of values. *Radiology* 2000;217:572–5.
102. Yoshioka J, Hasegawa S, Yamaguchi H, Tokita N, Paul AK, Xiuli M, et al. Left ventricular volumes and ejection fraction calculated from quantitative electrocardiographic-gated <sup>99m</sup>Tc-tetrofosmin myocardial SPECT. *J Nucl Med* 1999;40:1693–8.
103. Sharir T, Germano G, Kang X, Lewin HC, Miranda R, Cohen I, et al. Prediction of myocardial infarction versus cardiac death by gated myocardial perfusion SPECT: risk stratification by the amount of stress-induced ischemia and the poststress ejection fraction. *J Nucl Med* 2001;42:831–7.
104. Acampa W, Cuocolo A, Petretta M, Bruno A, Castellani M, Finzi A, et al. Tetrofosmin imaging in the detection of myocardial viability in patients with previous myocardial infarction: comparison with sestamibi and Tl-201 scintigraphy. *J Nucl Cardiol* 2002;9:33–40.
105. Peix A, Lopez A, Ponce F, Morales J, de la Vega AR, Chesa CS, et al. Enhanced detection of reversible myocardial hypoperfusion by technetium 99m-tetrofosmin imaging and first-pass radionuclide angiography after nitroglycerin administration. *J Nucl Cardiol* 1998;5:469–76.
106. Greco C, Ciavolella M, Tanzilli G, Sinatra R, Macrina F, Schillaci O, et al. Preoperative identification of viable myocardium: effectiveness of nitroglycerine-induced changes in myocardial sestamibi uptake. *Cardiovasc Surg* 1998;6:149–55.
107. Cerqueira MD. The user friendly nuclear cardiology report: what needs to be considered and what needs to be included. *J Nucl Cardiol* 1996;3:350–6.
108. Wackers FJT. Intersocietal Commission for the Accreditation of Nuclear Medicine Laboratories (ICANL) position statement on standardization and optimization of nuclear cardiology reports. *J Nucl Cardiol* 2000;7:397–400.
109. Germano G, Berman DS. Quantitative gated perfusion SPECT. In: Germano G, Berman DS, editors. *Clinical cardiac SPECT*. Armonk, NY: Futura Publishing Company; 1999. p. 115–46.
110. Pennell DJ, Prvulovich E. Image interpretation. In: Ell PJ, editor. *Nuclear cardiology*. London: British Nuclear Medicine Society; 1995. p. 56–79.
111. American Heart Association, American College of Cardiology, and Society of Nuclear Medicine. Standardisation of cardiac tomographic imaging. *Circulation* 1992;86:338–9.
112. Candell-Riera J, Santana-Boado C, Bermejo B, Armadans L, Castell J, Casans I, et al. Interhospital observer agreement on interpretation of exercise myocardial Tc-99m-tetrofosmin SPECT studies. *J Nucl Cardiol* 2001;8:49–57.
113. Knuuti J, Schelbert HR, Bax JJ. The need for standardisation of cardiac FDG PET imaging in the evaluation of myocardial viability in patients with chronic ischaemic left ventricular dysfunction. *Eur J Nucl Med Mol Imaging* 2002;29:1257–66.
114. Knuuti MJ, Nuutila P, Ruotsalainen U, Saraste M, Harkonen R, Ahonen A, et al. Euglycemic hyperinsulinemic clamp and oral glucose load in stimulating myocardial glucose utilization during positron emission tomography. *J Nucl Med* 1992;33:1255–62.
115. Berry JJ, Baker JA, Pieper KS, Hanson MW, Hoffman JM, Coleman RE. The effect of metabolic milieu on cardiac PET imaging using fluorine-18-deoxyglucose and nitrogen-13-ammonia in normal volunteers. *J Nucl Med* 1991;32:1518–25.
116. Knuuti MJ, Yki-Jarvinen H, Voipio-Pulkki LM, Maki M, Ruotsalainen U, Harkonen R, et al. Enhancement of myocardial [fluorine-18]fluorodeoxyglucose uptake by a nicotinic acid derivative. *J Nucl Med* 1994;35:989–98.
117. Schinkel AF, Bax JJ, Valkema R, Elhendy A, van Domburg RT, Vourvouri EC, et al. Effect of diabetes mellitus on myocardial <sup>18</sup>F-FDG SPECT using acipimox for the assessment of myocardial viability. *J Nucl Med* 2003;44:877–83.
118. Schroder O, Hor G, Hertel A, Baum RP. Combined hyperinsulinaemic glucose clamp and oral acipimox for optimizing metabolic conditions during <sup>18</sup>F-fluorodeoxyglucose gated PET cardiac imaging: comparative results. *Nucl Med Commun* 1998;19:867–74.

119. Lewis P, Nunan T, Dynes A, Maisey M. The use of low-dose intravenous Insulin in clinical myocardial F-18 FDG PET scanning. *Clin Nucl Med* 1996;21:15–8.
120. McCord ME, Bacharach SL, Bonow RO, Dilsizian V, Cuocolo A, Freedman N. Misalignment between PET transmission and emission scans: its effect on myocardial imaging. *J Nucl Med* 1992;33:1209–14. (discussion 1214–5).
121. Imaging guidelines for nuclear cardiology procedures, part 2. American Society of Nuclear Cardiology. *J Nucl Cardiol* 1999;6:G47–84.
122. Porenta G, Kuhle W, Czernin J, Ratib O, Brunken RC, Phelps ME, et al. Semiquantitative assessment of myocardial blood flow and viability using polar map displays of cardiac PET images. *J Nucl Med* 1992;33:1628–36.
123. Nekolla S, Miethaner C, Nguyen N, Ziegler S, Schwaiger M. Reproducibility of polar map generation and assessment of defect severity and extent assessment in myocardial perfusion imaging using positron emission tomography. *Eur J Nucl Med* 1998;25:1313–21.
124. Bergmann SR, Herrero P, Markham J, Weinheimer CJ, Walsh MN. Non-invasive quantitation of myocardial blood flow in human subjects with oxygen-15 labelled water and positron emission tomography. *J Am Coll Cardiol* 1989;14:639–52.
125. Choi Y, Huang SC, Hawkins RA, Kuhle WG, Dahlbom M, Hoh CK, et al. A simplified method for quantification of myocardial blood flow using nitrogen-13-ammonia and dynamic PET. *J Nucl Med* 1993;34:488–97.
126. Hutchins G, Schwaiger M, Rosenspire K, Krivokapich J, Schelbert H, Kuhl D. Noninvasive quantification of regional myocardial blood flow in the human heart using N-13 ammonia and dynamic positron emission tomographic imaging. *J Am Coll Cardiol* 1990;15:1032.
127. Iida H, Kanno I, Takahashi A, Miura S, Murakami M, Takahashi K, et al. Measurement of absolute myocardial blood flow with H<sub>2</sub><sup>15</sup>O and dynamic positron emission tomography. Strategy for quantification in relation to the partial-volume effect. *Circulation* 1988;78:104–15.
128. Muzik O, Beanlands R, Wolfe E, Hutchins GD, Schwaiger M. Automated region definition for cardiac nitrogen-13-ammonia PET imaging. *J Nucl Med* 1993;34:336–44.
129. Herrero P, Markham J, Shelton ME, Weinheimer CJ, Bergmann SR. Noninvasive quantification of regional myocardial perfusion with rubidium-82 and positron emission tomography. *Circulation* 1990;82:1377–86.
130. Di Carli M, Czernin J, Hoh CK, Gerbaudo VH, Brunken RC, Huang SC, et al. Relation among stenosis severity, myocardial blood flow, and flow reserve in patients with coronary artery disease. *Circulation* 1995;91:1944–51.
131. Uren NG, Melin JA, De-Bruyne B, Wijns W, Baudhuin T, Camici PG. Relation between myocardial blood flow and the severity of coronary-artery stenosis. *N Engl J Med* 1994;330:1782–8.
132. Gropler RJ, Lee KJ, Moerlein SM, Siegel BA, Geltman EM. Regional variation in myocardial accumulation of <sup>18</sup>F-fluorodeoxyglucose in fasted normal subjects. *J Am Coll Cardiol* 1990;15:81A.
133. Choi Y, Hawkins RA, Brunken RC, Huang SC, Kuhle WG, Chen K, et al. Evaluation of regional heterogeneity of myocardial glucose metabolism in normal humans using dynamic FDG-PET (abstract). *J Nucl Med* 1991;32:938.
134. Maes A, Flameng W, Borgers M, Nuyts J, Ausma J, Bormans G, et al. Regional myocardial blood flow, glucose utilization and contractile function before and after revascularization and ultrastructural findings in patients with chronic coronary artery disease. *Eur J Nucl Med* 1995;22:1299–305.
135. Mesotten L, Maes A, Herregods MC, Desmet W, Nuyts J, Van de Werf F, et al. PET “reversed mismatch pattern” early after acute myocardial infarction: follow-up of flow, metabolism and function. *Eur J Nucl Med* 2001;28:466–71.
136. Di Carli MF, Asgarzadie F, Schelbert HR, Brunken RC, Laks H, Phelps ME, et al. Quantitative relation between myocardial viability and improvement in heart failure symptoms after revascularization in patients with ischemic cardiomyopathy. *Circulation* 1995;92:3436–44.
137. Bax JJ, Poldermans D, Elhendy A, Cornel JH, Boersma E, Rambaldi R, et al. Improvement of left ventricular ejection fraction, heart failure symptoms and prognosis after revascularization in patients with chronic coronary artery disease and viable myocardium detected by dobutamine stress echocardiography. *J Am Coll Cardiol* 1999;34:163–9.
138. vom Dahl J, Althoefer C, Sheehan FH, Buechin P, Uebis R, Messmer BJ, et al. Recovery of regional left ventricular dysfunction after coronary revascularization. Impact of myocardial viability assessed by nuclear imaging and vessel patency at follow-up angiography. *J Am Coll Cardiol* 1996;28:948–58.
139. Choi Y, Hawkins RA, Huang SC, Gambhir SS, Brunken RC, Phelps ME, et al. Parametric images of myocardial metabolic rate of glucose generated from dynamic cardiac PET and 2-[<sup>18</sup>F]fluoro-2-deoxy-D-glucose studies. *J Nucl Med* 1991;32:733–8.
140. Gambhir SS, Schwaiger M, Huang SC, Krivokapich J, Schelbert HR, Nienaber CA, et al. Simple noninvasive quantification method for measuring myocardial glucose utilization in humans employing positron emission tomography and fluorine-18 deoxyglucose. *J Nucl Med* 1989;30:359–66.
141. Blanksma PK, Willemsen AT, Meeder JG, de Jong RM, Anthonio RL, Pruim J, et al. Quantitative myocardial mapping of perfusion and metabolism using parametric polar map displays in cardiac PET. *J Nucl Med* 1995;36:153–8.